AD-A014 926

NORWEGIAN SEISMIC ARRAY (NORSAR) PHASE 3

K. A. Berteussen

Royal Norwegian Council for Scientific and Industrial Research

Prepared for:

Air Force Technical Applications Center
Advanced Research Projects Agency

8 August 1975

273093

NORSAR ROYAL NORWEGIAN COUNCIL FOR SCIENTIFIC AND INDUSTRIAL RESEARCH

ADA014926

Scientific Report No. 5-74/75

FINAL TECHNICAL REPORT
NORSAR PHASE 3

1 July 1974 – 30 June 1975

Prepared by
K. A. Berteussen

D D C

SEP 19 1975

C

Kjeller, 8. August 1975

Sponsored by
Advanced Research Projects Agency
ARPA Order No. 2551

REPORT DOCUMENTATION PAGE

READ INSTRUCTIONS
BEFORE COMPLETING FORM

1. REPORT NUMBER	2. GOVT ACCESSION NO.	3. RECIPIENT'S CATALOG NUMBER
F08606-74-C-0049		

4. TITLE *(and Subtitle)*	5. TYPE OF REPORT & PERIOD COVERED
Final Report - NORSAR Phase 3 1 July 1974 - 30 June 1975	Technical Report 1 July 74 - 30 June 75
	6. PERFORMING ORG. REPORT NUMBER Sci. Rep. No. 5-74/75

7. AUTHOR(s)	8. CONTRACT OR GRANT NUMBER(s)
K.A. Berteussen (editor)	F08606-74-C-0049

9. PERFORMING ORGANIZATION NAME AND ADDRESS	10. PROGRAM ELEMENT, PROJECT, TASK AREA & WORK UNIT NUMBERS
NTNF/NORSAR Post Box 51 2007 Kjeller, Norway	NORSAR Phase 3

11. CONTROLLING OFFICE NAME AND ADDRESS	12. REPORT DATE
Vela Seismological Center 312 Montgomery Street Alexandria, Va. 22314	8 August 1975
	13. NUMBER OF PAGES 114

14. MONITORING AGENCY NAME & ADDRESS(*if different from Controlling Office*)	15. SECURITY CLASS. *(of this report)*
	15a. DECLASSIFICATION DOWNGRADING SCHEDULE

16. DISTRIBUTION STATEMENT *(of this Report)*

Approved for public release; distribution unlimited.

17. DISTRIBUTION STATEMENT *(of the abstract entered in Block 20, if different from Report)*

18. SUPPLEMENTARY NOTES

19. KEY WORDS *(Continue on reverse side if necessary and identify by block number)*

NORSAR, Seismic Array, Seismology

20. ABSTRACT *(Continue on reverse side if necessary and identify by block number)*

This report covers research and operation activities at the Norwegian Seismic Array (NORSAR) for the period 1 July 1974 - 30 June 1975. The research activities are described in chapters A-S, while chapters T-Y report on data processing, programming, ARPANET activities, computer center operation and array maintenance.

DD FORM 1473 EDITION OF 1 NOV 65 IS OBSOLETE
1 JAN 73

AFTAC Project Authorization No.:   VT/5702/B/ETR

TABLE OF CONTENTS

TABLE OF CONTENTS

(Cont.)

SUMMARY

This report covers research and operation activities
at the Norwegian Seismic Array (NORSAR) for the period
1 July 1974-30 June 1975. The research activities are
described in chapters A-S, while chapters T-Y report on
data processing, programming, ARPANET activities, computer
center operation and array maintenance.

In the reporting period seismological research covering
a wide range of topics has been going on at NORSAR. Some
projects are continued from the previous period, while some new
projects represent topics previously not covered by this institu-
tion. Scattering of teleseismic signals has been given a
great deal of attention the last few years both at NORSAR
and other institutions. Chapters A, B and C represent a
continuation of previous work in this field, while
Chapter H discusses the effect of scattering of signals
from local events. The location of the source of array-
recorded slowness, azimuth and internal time anomalies
has been discussed ever since they first were discovered.
In Chapters D and E it is demonstrated that both for
NORSAR and LASA these are mainly of local origin. The
details of the local structure causing these anomalies
are investigated 3-dimensionally in Chapter F, while the
next Chapter (G) reports on a study of the upper mantle
in the vicinity of the NORSAR array.

A new method for a parameterized description of both seis-
mic signals (Chapter I) and noise (Chapter J) is presented.
Chapter K reports on an earthquake/explosion discrimination
study using the $m_b:M_s$ method, while it is demonstrated in
Chapter L that the method described in Chapters I and J
can be used to improve the discrimination capability of
the array. The 'Kirnos project' for comparison of 'east'
and 'west' magnitudes is now finished and the results
are presented in Chapter M. Chapter N is a report on the
problem of using various statistical tests for discriminating

between seismic noise and signals.

Chapters O, P and Q are devoted to surface wave studies.
The first of these (Chapter O) is a study of surface
wave dispersion between Kirkenes and Kings Bay. The second
one (Chapter P) is a study of anisotropy using higher
mode surface waves, while the last (Chapter Q) is a study
of source spectra and scaling laws.

In Chapter R it is demonstrated that seismic 'noise'
produced by a hydroelectric power plant may be used for
studies of in situ stress. The last of the research chapters
(S) is a study of the seismicity in Fennoscandia.

Chapters T-Y report on the operation of the array.
Chapters T and U describe the event detection and processing
activities. It is demonstrated that previous research
efforts reported herein has successfully been included in
the daily operation. Although the programming staff has
been reduced, Chapter V can report on a large activity
of this group in several fields. One such example is
their work on the ARPANET (Chapter W) which has become
an integrated part of the NORSAR daily life. Chapters
X and Y report on the operation of the data center and
the array maintenance, respectively.

K.A.Berteussen

A.   STUDIES OF PRECURSORS

The correct interpretation of precursor signals associated
with the seismic phases PP, PKIKP, PKPPKP and others has
an important bearing on the delineation of structure within
the Earth . Of particular importance is the problem
of identifying and analysing seismic waves which have
resulted by scattering by small-scale
random irregularities in density and elastic parameters
inside the Earth. Many previous studies of precursors have
implicitly discriminated against the possibility of scatter-
ing type interpretations in their data selection and analysis
methods. Experiments capable of discriminating between
scattering and other possible interpretations of precursor
signals on the basis of estimates of the slownesses and
azimuths of the various arrivals must necessarily involve
array data sampled densely and simultaneously in space.

A.1   Processing of Seismic Precursor Data

A program (BEAMAN) has been developed which calculates
continuously beam power/second over a symmetrical dense
grid of slowness-azimuth values. This processing procedure
has two main attributes in the analysis of precursor signals.
Firstly, significant peaks in the power distribution images
provide robust estimates of slowness, azimuth and time even
for the small and variable signals generally encountered
in precursor wave trains. In many cases the concordance
or discordance of these estimates with theoretical expecta-
tions can, even after generous allowance is made for measure-
ment uncertainties, discriminate sharply between scattering
and alternative (deterministic) interpretations. The second
attribute of the processing method used is that it yields
a continuous three dimensional mapping of the power distri-
bution; this is additionally valuable insofar as the distri-
bution of any power subsidiary to the major power peaks

can potentially substantiate a scattering interpretation
but generally finds no explanation in alternative hypotheses.
Conventional least squares methods for estimating slowness
and azimuth essentially rely on signal energy being highly
concentrated in slowness-azimuth space and yield only discrete
slowness-azimuth estimates. In consequence, such methods are
not fully appropriate for the analysis of signals having
a potential scattering origin. An example of a beam power
plot in slowness-azimuth space is shown in Fig. A.2.

<div style="text-align: right">

D.W. King, E.S. Husebye,
R.A.W. Haddon

</div>

A.2   Precursors to PP

A detailed study of so-called precursors to PP $(90^{\circ} \lesssim \Delta \lesssim 110^{\circ})$
has been completed (King et al, 1975). In summary, the
results of a theoretical study of the interpretation of
the precursors in terms of scattering by small-scale
random irregularities in the crust and uppermost mantle
have been compared with observational data from 2 nuclear
explosions recorded at the Warramunga array and 3 earth-
quakes recorded at the NORSAR array. The NORSAR data com-
prises mainly onset times and duration, slowness, azimuth
and amplitude variations determined using BEAMAN analysis
of precursor wave trains such as those illustrated in Fig.
A.1. The comparison of theoretical and observational results
reveals that the scattering interpretation offers a plausible
and adequate explanation of the detailed observational data.
In contrast, previous interpretations fail to account for
the extended duration of observed wave trains, and for the
wide azimuthal distribution of energy incident at the re-
ceiver. The scattering interpretation of PP precursors
removes the need for postulating many sharp reflecting
discontinuities in the uppermost few hundred kilometers
of the crust and upper mantle.

<div style="text-align: right">

D.W. King, R.A.W. Haddon,
E.S. Husebye

</div>
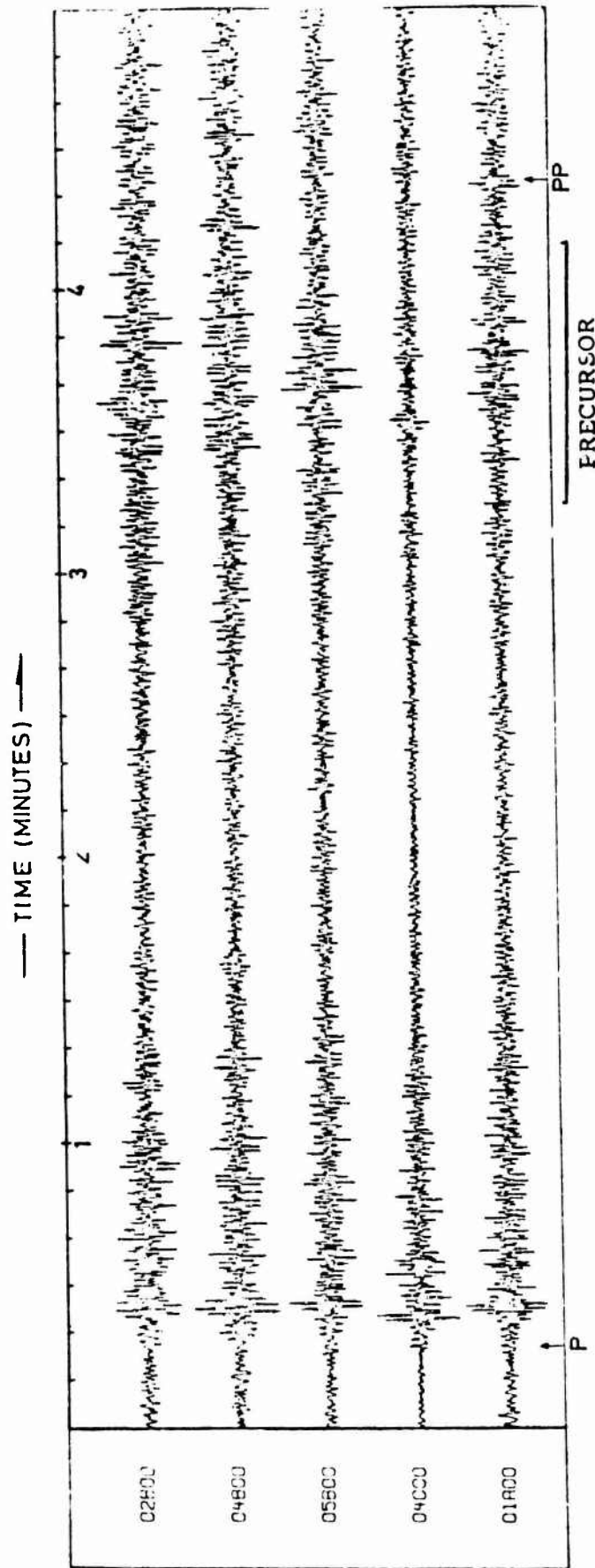
Fig. A.1   Seismograms from 5 selected subarray central instruments (as labelled) for
an event in Molucca Passage ($\Delta \sim 100°$). The traces have been filtered in the
range 0.6-3.0 Hz. Note the extended duration and variable nature of PP
precursor wave train.

A.3 Precursors to PKIKP

The distribution of slowness, azimuth and amplitude along
PKIKP precursor wave trains ($125^{O} \lesssim \Delta \lesssim 143^{O}$) recorded at NORSAR
has been investigated and shown to be fully consistent with
that entailed by a theoretical treatment of the scattering
of P waves by small-scale random inhomogeneities in the
lowest mantle near where P waves enter into and exit from
the core. It has been established that the azimuth of arrival
of precursor energy can migrate with increasing time from
values near to the primary PKP azimuth to values differing
from the PKP azimuth by as much as 30°. The migration of
peak precursor beam power in both slowness and time is
illustrated in the consecutive frames of Fig. A.2. The
theoretical slowness-azimuth distribution entailed by
scattering at the mantle-core boundary is superimposed
on this figure, and the agreement between observed and
predicted values is remarkably good. In marked contrast
with the precursor data, the main PKIKP arrivals are stable
and compact over several seconds. These and similar data
are particularly strong evidence in support of a scattering
interpretation. Furthermore, they discriminate sharply
against traditional interpretations involving transition
layers within the outer core. Since in addition data pre-
viously interpreted as corroborating the existence of sharp
reflecting discontinuities within the outer core can be
adequately accounted for on the scattering interpretation,
there appears to be no seismological evidence which requires
distinct layering of the Earth's outer core.

E.S. Husebye, D.W. King,
R.A.W. Haddon

A.4 Precursors to PKPPKP

Seismic scattering by small-scale random inhomogeneities
in the lower and upper mantle has already been
shown to account for observed precursors to the
seismic phases PKIKP and PP. The theoretical implications
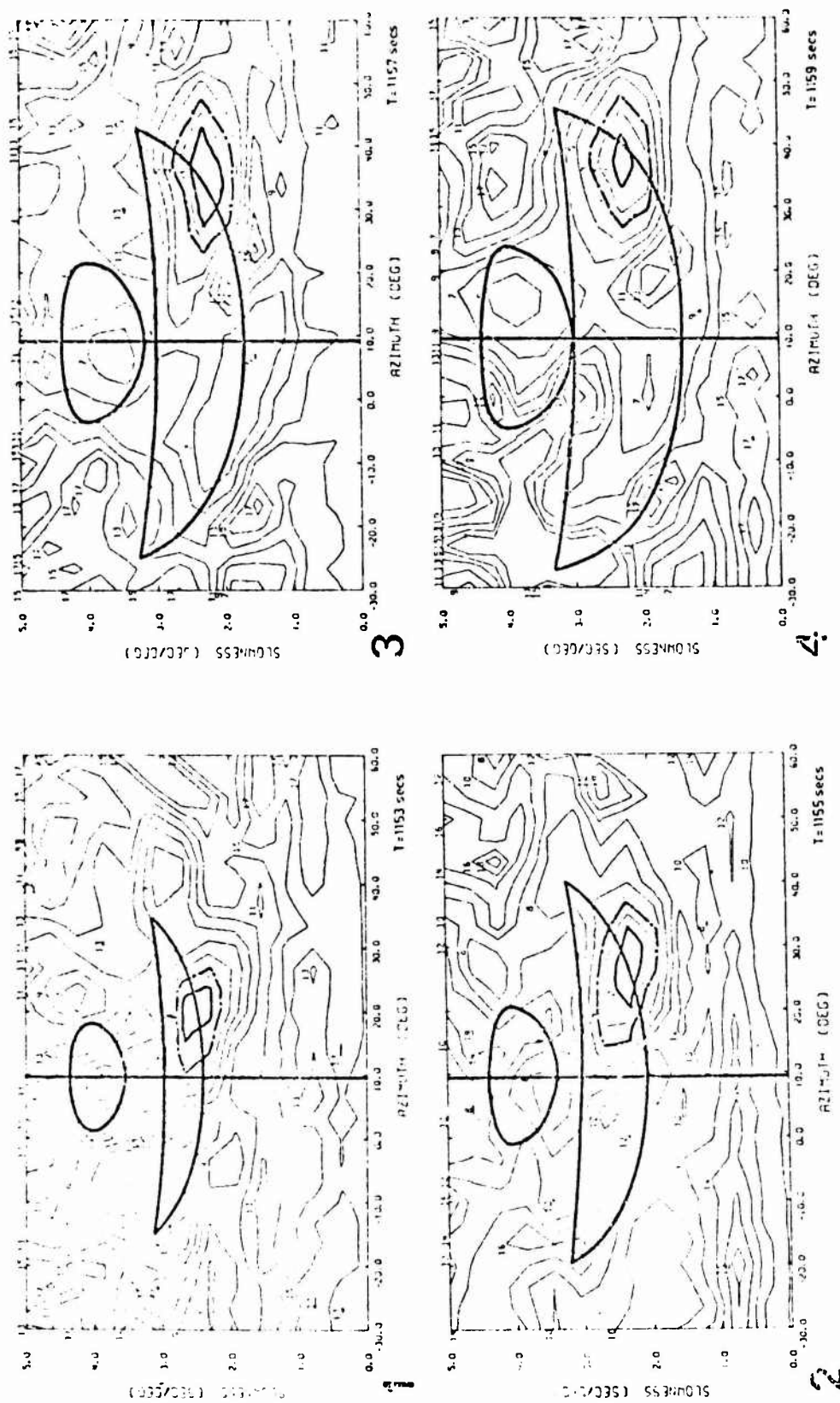
Fig. A.2 Contoured beam power levels in slowness-azimuth space for continguous 2 second intervals of PKIKP precursors with mean corrected travel times as indicated for an event at Δ=135.7°. The contours represent power levels in dB below a maximum of 25.7 dB. Contours enclosing dominant peaks in each frame are darkened. Theoretical slowness-azimuth curves for scattered waves of corresponding travel time are plotted centered on the measured primary PKP azimuth.

of these random inhomogeneities in respect of scattering of P'P' phases are being examined in detail and compared with observational data on P'P' precursors at NORSAR. It has been found that observed P'P' precursors having lead times up to about 50 seconds before the main P'P' phases are consistent with having the same scattering origins as precursors to PP and PKIKP. As with the scattering inter-pretation of precursors to PP, the scattering interpretation of precursors to P'P' removes the need for postulating certain reflecting discontinuities in the upper mantle.

<div align="right">

R.A.W. Haddon, E.S. Husebye
D.W. King

</div>

Synopsis of precursor studies compiled by D.W.King.

REFERENCES

R.A.W. Haddon, E.S. Husebye, D.W. King. Origins of precursors to P'P', manuscript in preparation.

E.S. Husebye, D.W. King, R.A.W. Haddon. Precursors to PKIKP and scatter-ing near the mantle-core boundary, submitted for publication.

D.W. King, E.S. Husebye, R.A.W. Haddon. Precursors to PP, Phys. Eartn Planet. Int., in press.

D.W. King, E.S. Husebye, R.A.W. Haddon. Processing of seismic precursor data, manuscript in preparation.

B. WAVE SCATTERING THEORY IN ANALYSIS OF P-WAVE ANOMALIES
    AT NORSAR AND LASA

Observed travel time and amplitude anomalies at the NORSAR
and LASA arrays are significantly larger than the measurement
errors, and cannot be explained in terms of deterministic
crust and upper mantle structural models for the respective
siting areas. In this study (Berteussen et al, 1975) the
Chernov (1960) theory has been used in modelling the crust
and upper mantle as a random medium, and also to estimate
to what extent such models can account for the observed
anomalies. In Table B.1 the basic assumptions underlying
the Chernov (1960) theory for acoustical wave propagation
in random media is summarized, while Tables B.2 and B.3
show the results obtained for the crust and upper mantle
under NORSAR and LASA respectively. It is found that the
random medium modelling can explain 50 to 60% of the variance
of the time and amplitude anomalies at NORSAR. The correspond-
ing results for LASA are 50-60% and 25% respectively. In
contrast, reasonable deterministic models cannot account
for even 25% of this variance. While the random medium
model can provide a satisfactory explanation of the observa-
tional data, extensive tests have revealed that the para-
meters characterizing the random medium cannot be uniquely
determined from the data.

K.A. Berteussen, A. Christoffersson,
E.S. Husebye, A. Dahle

REFERENCES

Aki, K. (1973): Scattering of P-waves under the Montana LASA, J. Geophys.
    Res., 78, 1334-1346.

Berteussen, K.A., A. Christoffersson, E.S. Husebye and A. Dahle (1975):
    Wave scattering theory in analysis of P-wave anomalies at NORSAR
    and LASA, Geophys. J.R. Astr. Soc., in press.

Capon, J. (1974): Characterization of crust and upper mantle structure
    under LASA as a random medium, Bull. Seism. Soc. Am., 64, 235-266.

Chernov, L. (1960): Wave propagation in random media, trans. by
    R.A. Silverman, McGraw-Hill Book Company, New York.

TABLE B.1

Basic assumptions underlying the Chernov (1960) theory for
acoustical wave propagation in random media.

1. Small velocity variations, $\overline{\mu^2} \ll 1$

2. Statistically homogeneous

3. Statistically isotropic

4. Gaussian correlation function for index of
    refraction, $N(r) = e^{-r^2/a^2}$

5. Extent of medium much greater than correlation
    distance, $L \gg a$

6. Large scale inhomogeneities (Fresnel-approximation)
    $ka \gg 1$

7. Rytov (Born) approximation
    $\frac{\Delta I}{I} \ll 1$ per wavelength (for the whole medium

TABLE B.2

Results obtained in modelling the crust and upper mantle beneath NORSAR as a Chernov medium. An asterisk indicates that the standard deviation of the refractive index corresponds to the lower limit of the extent of the medium.

DATA		CHERNOV MEDIUM MEASUREMENT			
Configuration	Amp/phase	S.d. of refraction index (%)	Correlation Distance (km)	Extent of Medium (km)	Variance Reduction (%)
1A,1B	P	1.6*	17	> 100	97
2B,3B	P	0.8	12	300	84
1B,7B	P	1.0	16	250	96
4B,5B	P	0.9	18	200	93
1A,6B	P	0.9	25	350	96
1A,1B	A	1.2	14	100	60
2B,3B	A	1.4	15	100	57
1B,7B	A	1.3*	8	> 250	36
4B,5B	A	1.0*	> 25	> 250	20
1A,6B	A	1.0*	17	> 150	60
1A,1B-4B	P	0.5	30	> 250	71
1A,1B-4B	A	0.9	30	≥ 250	73
1A,1B-7B	P	2.0	60	≥ 250	66
1A,1B-7B	A	0.8	35	≥ 100	60

TABLE B.3

Results obtained in modelling the crust and upper mantle beneath LASA as a Chernov random medium. Corresponding results obtained by Aki (1973) and Capon (1974) are also given.

DATA		CHERNOV MEDIUM MEASUREMENTS			
Configuration	Amp/Phase	S.d. of refraction index (%)	Correlation Distance (km)	Extent of Medium (km)	Variance Reduction (%)
A0,B1,B4	P	0.6 0.3	15	50 150	25
A0,B1,B4	A	3.0 2.0	15	50 150	58
66 instruments (Aki, 1973)	A&P	4.0	10	60	
A,B,C ring (Capon, 1974)	A&P	2.0	12	120	

C.   TIME AND AMPLITUDE FLUCTUATIONS OF TELESEISMIC P-SIGNALS
      AT NORSAR IN VIEW OF WAVE SCATTERING THEORY

In the study of Berteussen et al (1975) it was demonstrated
that a considerable part of the time and amplitude anomalies
observed at the large seismic arrays can be explained using
the Chernov (1960) theory for wave propagation in a random
medium. In this study (Dahle, 1975) more emphasis is given
to the theoretical aspect of applying this theory and on
the validity of doing so. There is limited success with
regard to the proposed scattering hypothesis; however, it
is believed that the scattering approach deserves consider-
able attention. Such a conclusion is justified by the
fact that the seismic wave field exhibits to a satisfactory
degree some of the statistical qualities predicted by the
theory. For example, the theory predicts a positive corre-
lation between phase and amplitude anomalies, which also is
observed. The assertion of forward wave scattering and mode
conversion being basically P→P turns out to be an important
point. There is reason to suspect the crust and upper mantle
locally being inhomogeneous in a way not pertaining to
Chernov's (1960) theory for weak inhomogeneities equally
distributed throughout the medium. Stronger inhomogeneities
giving rise to back-scattering, conversion to modes other
than P and higher order scattering (scattered-scattered
waves) are possible explanations of an observed discrepancy
between theory and experience.

Substantial support to the scattering hypothesis is provided
by the correlation functions depicted in Fig. C.1, which
shows the correlation of time and amplitude anomalies
respectively as a function of spatial lag. These are the
features leading to the space predictive procedure described
in Quarterly Report no. 3 in 1973. The prediction procedure
is important for two reasons. Firstly, because it shows the
anomaly percentage explainable by correlated stochastic
terms, and secondly it provides a means of finding the
optimum correlation matrix for the data.

(a)

(b)
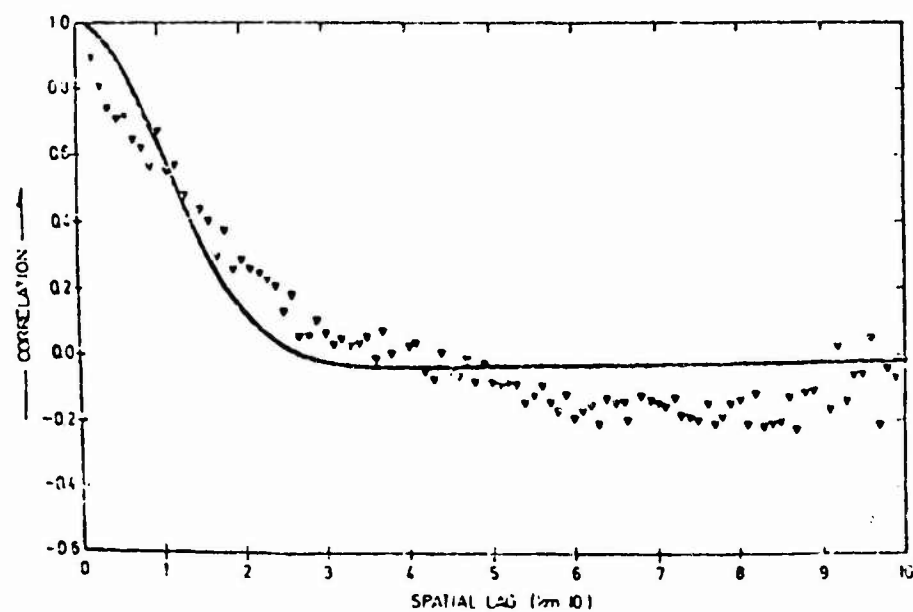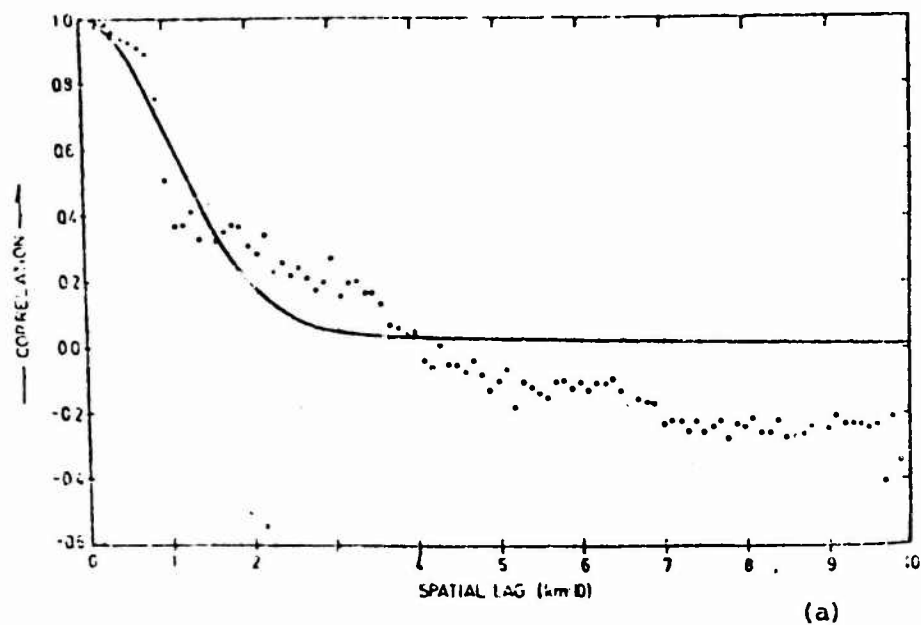
.Fig..C.1 Empirical transverse correlation functions for travel time
fluctuations (a) and logamplitude fluctuations (b) together
with the theoretical Chernov (1960) functions with correlation
distance 15 km and wave parameter 10.

The realization of randomly corrugated seismic wave fronts
is undoubtedly important in small aperture array seismology.
In this study one has successfully related the fluctuations
in body wave travel time, local wave front normal and ampli-
tude to wave scattering in an inhomogeneous crust and upper
mantle. A quantitative description of the inhomogeneous
medium is inconclusive for the moment, but the results
show that attention must be paid to scattering effects when
observed times or amplitudes are inverted into structural
models.

A. Dahle

REFERENCES

Berteussen, K.A., A. Christoffersson, E.S. Husebye and A. Dahle (1975):
Wave scattering theory in analysis of P-wave anomalies at NORSAR
and LASA, Geophys. J.R. Astr. Soc., in press.

Chernov, L. (1960): Wave propagation in random media, trans. by R.A.
Silverman, McGraw-Hill Book Company, New York.

Dahle, A. (1975): Time and amplitude fluctuations of teleseismic P-signals
at NORSAR in view of wave scattering theory, Scientific Report
No. 4-74/75, NTNF/NORSAR, in press.

D.   ON THE ORIGIN OF SLOWNESS AND AZIMUTH ANOMALIES OF TELE-
     SEISMIC SIGNALS

Using slowness and azimuth anomalies observed from P and PKP
phases at NORSAR, it has been demonstrated (Berteussen, 1975)
that as much as 90% of the corresponding anomalies for PP and
PcP phases can be predicted. It is thus concluded that ano-
malies caused by inhomogeneities at the source side or at
the deepest part of the ray path cannot be observed at NORSAR,
i.e., for PP phases inhomogeneities on the source side of
the surface reflection point and for PcP phases inhomogeneities
on the source side or at the mantle-core reflection point are
not strong enough to produce anomalies which can be identi-
fied in this type of data. Even after having corrected for
the first order effect of the local structure (a dipping
plane interface), there is no significant part of the ano-
malies left that can be ascribed to inhomogeneities at the
source side. It has further been demonstrated that locating
a significant part of the anomalies deep in the mantle would
require unreasonable velocity contrasts; one thus has to
conclude that most of these anomalies are caused by structures
in the very upper part of the mantle or in the crust.

An additional piece of information (Berteussen, 1975) has been
time residual and wave front slowness and azimuth measurements
of long period P-waves inside three different frequency
bands, 0.1 Hz highpass, all pass, and 0.05-0.1 Hz bandpass.
It is found that the location error vectors gradually
diminish as the frequency decreases. For the 0.1 Hz highpass
data the vectors are essentially the same as for short period
data, and then they change to about half the size but keep
their direction for the longest wavelengths. Assuming that
the linear extent of structures causing measurable anomalies
have to be, say at least half a wavelength, it is thus found
that since the longest wavelengths used (160-80 km) have 58%

of the (dT/dΔ, Φ) anomalies of the short period data, 58%
of these have to be caused by inhomogeneities with a linear
extent of at least say $1/2$ $(\frac{160+80}{2})$ = 60 km. Then there are
42% of the anomalies which these long waves do not 'see',
thus indicating that the inhomogeneities causing these
anomalies must have a linear extent too small for these
waves, i.e., 42% of the slowness and azimuth anomalies are
caused by inhomogeneities of linear extent less than 60 km.
From the 0.1 Hz highpass filtered data (wavelength ~ 80 km)
it is further concluded that 17% (75-58) of the anomalies
are caused by inhomogeneities of linear extent between 60
and 40 km. The remaining 25% of the slowness and azimuth
anomalies and virt· ly 100% of the plane wave front devia-
tions then have to oe caused by inhomogeneities which have
characteristic sizes of less than 4C km. It has been shown
(Berteussen, 1975) that at NORSAR the best plane wave front
reduces the variance of the time anomalies relative to
the wave front predicted from the PDE event location by
approximately 50% and that thus the time deviation around
this best plane wave front accounts for the remaining 50%.
If one therefore instead of thinking in terms of (dT/dΔ, Φ)
anomalies and plane wave front deviations thinks of time
deviations relative to the wave front predicted from the PDE
event location the following picture emerges. 29% (58/2) of
these are caused by inhomogeneities larger than 60 km, 9%
are caused by inhomogeneities between 60 km and 40 km, and
the remaining 62% $(\frac{100+25}{2})$ are caused by inhomogeneities of
size less than 40 km. From the previous section we know that
virtually all the anomalies are caused by inhomogeneities
in the very upper mantle under the receiver, say above 600 km.
We are now in a position to also set an upper limit to
these inhomogeneities. Assuming that the anomalies are caused
by structures as close to the receiver as possible, we find
that a maximum of 71% (62+9) of these are produced within
the last 40 km, and in order to include the remaining 29% we
then have to go down to a depth of at least 60 km.

<div align="right">K.A. Berteussen</div>

REFERENCES

Berteussen, K.A. (1975): The origin of slowness and azimuth anomalies
at large arrays, submitted for publication.

E.   THE EFFECT OF ARRAY CONFIGURATION ON SLOWNESS AND AZIMUTH
     ANOMALIES

The multitude of sensors characterizing the large seismic
arrays makes it possible to test what effect a change in
array configuration has on the slowness and azimuth anomalies
for P-phases recorded at the arrays. In two recent papers
this effect has been studied both for LASA (Berteussen, 1975a)
and NORSAR (Berteussen, 1975b).

On Fig. E.1 the 'array diagram' for a set of well-recorded
P-phases at LASA using all 21 subarrays is shown. The tail
of the arrows represents the slowness and azimuth (dT/dΔ, Φ)
estimated at the array, while the head represents the values
entailed by a (laterally homogeneous) standard earth model.
On Fig. E.2 the same array diagram is then shown when only
odd numbered LASA subarrays have been used. The configuration
is somewhat 'thinner' than the full array, but has approxi-
mately the same aperture (200 km). Comparing Figs. E.1 and
E.2, it is immediately apparent that certain sectors
(especially azimuth $90^{\circ} \lesssim \Phi \leq 270^{\circ}$) of the two array diagrams
are significantly different. In particular, the anomalies
associated with rays which bottom in the vicinity of proposed
plume structures under Hawaii ($\Phi \sim 265^{\circ}$) at LASA and the
Galapagos Islands ($\Phi \sim 155^{\circ}$) (Davies and Sheppard, 1972,
Kanasewich et al, 1973) are markedly different in the two
figures. Anomalies associated with rays bottoming in the
lowest mantle beneath Iceland ($\Phi \sim 20^{\circ}$) are essentially con-
sistent on Figs. E.1 and E.2; however, array diagrams for
other configurations (Berteussen, 1975a) demonstrate con-
clusively that these anomalies are also critically dependent
on the spatial sampling of the wavefront.

The same effects may also be demonstrated at NORSAR. On
Fig. E.3 the array diagram for the full NORSAR array is
shown, while Fig. E.4 shows a diagram using subarrays 1, 5-8,
15-20, giving us an array of aperture 70 km instead of the
100 km aperture of the whole NORSAR. For the azimuth section

330-120 degrees it is seen that the vectors have been rotated
by almost 90 degrees relative to those on Fig. E.3. Also
note that for azimuth 300 degrees (the direction to Iceland)
Fig. E.4 shows rapid variations in the anomaly pattern.
Given a NORSAR array consisting of only these eleven sub-
arrays, one could, following Davies and Sheppard (1972)
and Kanasewich et al (1973), be tempted to associate these
rapid changes with, for example, a hot spot under Iceland.
However, a more complete picture (Fig. E.3) demonstrates
that such an interpretation would be erroneous. Using
smaller arrays and fewer subarrays even more drastic
variations can of course be induced. On Fig. E.5 the
array diagram for the NORSAR subarray combination 2, 3, 9,
10, 11, giving an aperture of some 45 km, which still is
larger than most of the medium-sized arrays, is shown.
For the direction towards Iceland, the arrows are now seen
to be turned quite opposite to those on Fig. E.4. Also
for the rest of the slowness-space large differences are
observed relative to the data on Figs. E.3 and E.4. Finally,
(Fig. E.6) an array diagram is shown using only the subarrays
6, 17, 20. This configuration is approximately the same as
that of the Hagfors array in Sweden, and demonstrates that
for such a small array almost 'any' type of location errors
may be found. On Fig. E.6 one interesting detail should be
noted. One of the arrows (azimuth~0) is seen to be turned
in almost the same direction as the core phases between
azimuth 0° and 90°, and directly opposite to the surrounding
P-wave vectors, thus indicating that the anomaly for the core
phases is a function only of direction of approach of the ray.

Clearly, there are a lot of details in each of these figures
which it would be tempting to associate with structures far
away from the receiver. The fact that these details are not
retained as one changes configuration suggests, however,
that in reality the wavefronts are locally delayed or speeded
up for example by rapid Moho depth variations and/or scatter-
ing by small-scale randomly distributed inhomogeneities close

to the receiver. The final estimates of slowness and azimuth
are then very much dependent on which sites are sampled
and which are not. Of course, source side or deep mantle
effects may be present in the data, but local structural
effects have been shown to be so dominant and so difficult
to characterize (and therefore to correct for) that there
can be no justification for speculating on structures well
removed from the array on the basis of these data.

K.A. Berteussen

REFERENCES

Berteussen, K.A. (1975a): Array analysis of lateral inhomogeneities
in the deep mantle, submitted for publication.

Berteussen, K.A. (1975b): The origin of slowness and azimuth anomalies
at large arrays, submitted for publication.

Davies, K., and R.M. Sheppard (1972): Lateral heterogeneity in the
earth's mantle, Nature, 239, 318-323.

Kanasewich, E.R., R.M. Ellis, C.H. Chapman, P.R. Gutowski (1973):
Seismic array evidence of a core-boundary source for the
Hawaiian linear volcanic chain, J. Geophys. Res., 78, 1361-1371.

Direction to
Iceland

Direction to
The Galapagos Islands

Direction to
Hawaii
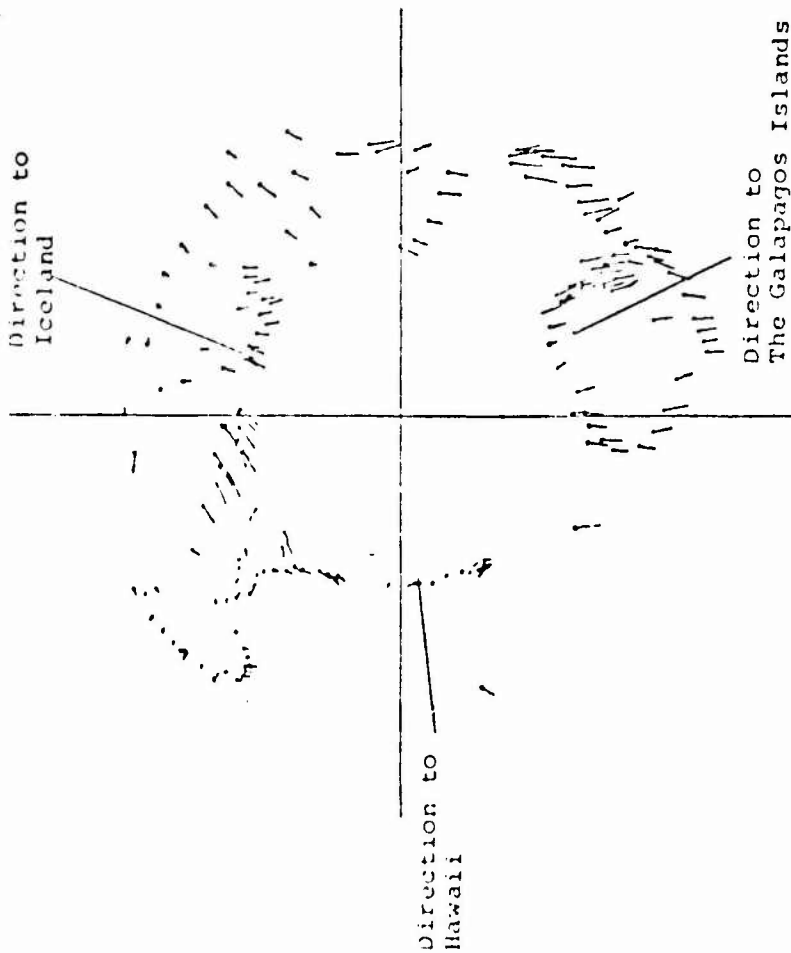
Fig. E.1 Array diagram for a configuration consisting
of all 21 LASA subarrays. The tail of the
arrows represents the observed (dT/dΔ, Φ),
i.e., the slowness-space location measured at
LASA. The head of the arrows represents the
(dT/dΔ, Φ) one expects using the PDE event
location and standard distance-slowness tables.
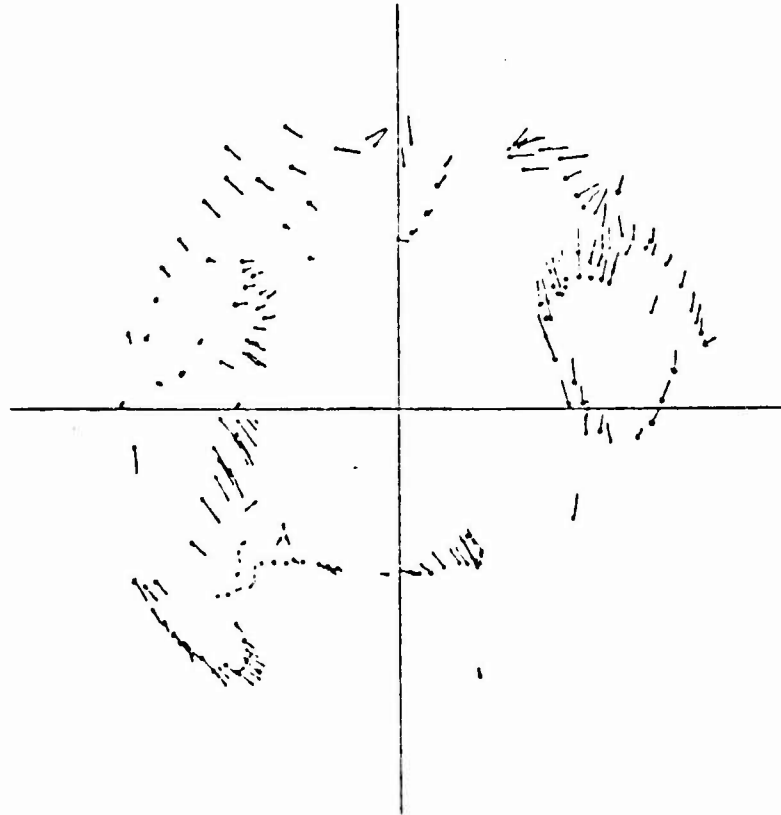
Fig. E.2 Same as Fig. E.1 for the LASA
subarrays 1,3,5,7,9,11,13,15,17,19,21
(A0,B2,B4,C2,C4,D2,D4,E2,E4,F2,F4).

Direction to
Iceland
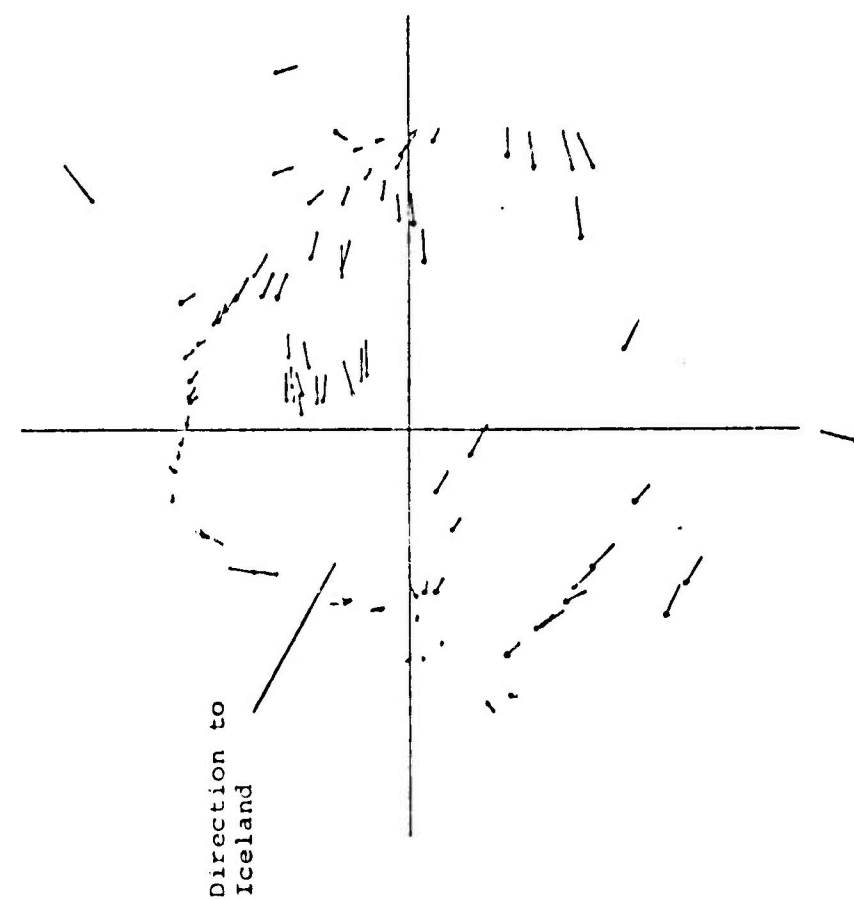
Fig. E.3   Same as Fig. E.1 for all 22 NORSAR subarrays.

Fig. E.4   Same as Fig. E.1 for the NORSAR
subarrays 1, 5-8, 15-20 (1A, 4B-7B,
7C-12C).

Fig. E.6   Same as Fig. E.1 for the NORSAR
subarrays 6, 17, 20 (5B, 9C,12C).

Fig. E.5   Same as Fig. E.1 for the NORSAR subarrays
2,3,9,10,11 (1B,2B,1C,2C,3C).

F. DETERMINATION OF THE THREE-DIMENSIONAL SEISMIC STRUCTURE OF THE LITHOSPHERE

A new three-dimensional earth modelling is formulated in order to meet an increasing demand for more detailed and accurate information about the earth's interior. We start with a layered medium of classic seismology, but divide each layer into many blocks and assign a parameter to each block which describes the velocity perturbation from the average for the layer. Our data is the teleseismic P travel time residuals observed at an array of seismographs distributed on the surface above the earth's volume we are modelling. By isolating various sources of errors and biases, we arrive at a system of equations to determine the model parameters. The solution was obtained by the use of generalized inverse and stochastic inverse methods with the analysis of resolution and errors in estimates. Our method also gives a lower limit of the true r.m.s. velocity fluctuation in the actual earth under the assumption of ray-theory.

Using NORSAR P-wave residuals, we have determined the three-dimensional seismic structure of the lithosphere under the array to the depth of 126 km. The true r.m.s. velocity fluctuation was found to be at least 3.4%. This is in agreement with estimates obtained from statistical analysis of P time fluctuation based on the Chernov theory. The three-dimensional velocity anomalies are presented both by the generalized inverse and by the stochastic inverse solutions. We preferred the dual presentation, because it gives the reader greater freedom in judging the results than a single "optimal" solution. Both methods gave essentially the same results. The discrepancies, when they existed, were always explainable in terms of differences in the smoothing procedure which is explicitly given in the resolution matrix.

We found clear evidence of pipe-like structures under NORSAR,
dipping northward and away from the surface contour of the Oslo
graben (Fig. F.1). These pipe-like structures were interpreted
as vestiges of magma ascent by penetrative convections
associated with the Permian volcanism of the Oslo graben.
The inclination of the pipe-like structures is interpreted
as a result of plastic deformation of the lithosphere due
to the shear exerted by the asthenosphere convection current
driving the plate motion.

In case of LASA, the most conspicuous feature of the estimated
three-dimensional velocity anomaly is a $N60^{O}E$ trend which per-
sists from the upper crust to depths greater than 100 km.
Relatively high velocities are found towards SE and low
velocities in the cenral array siting area and towards NW.
We are tempted to associate the $N60^{O}E$ trending velocity
anomalies with shearing caused by the Nevadan and Laramie
orogenies in the western United States. The shear may be
concentrated in a zone of weakness which in turn causes a
broad low velocity anomaly throughout the lithosphere.

K. Aki, A. Christoffersson
E.S. Husebye
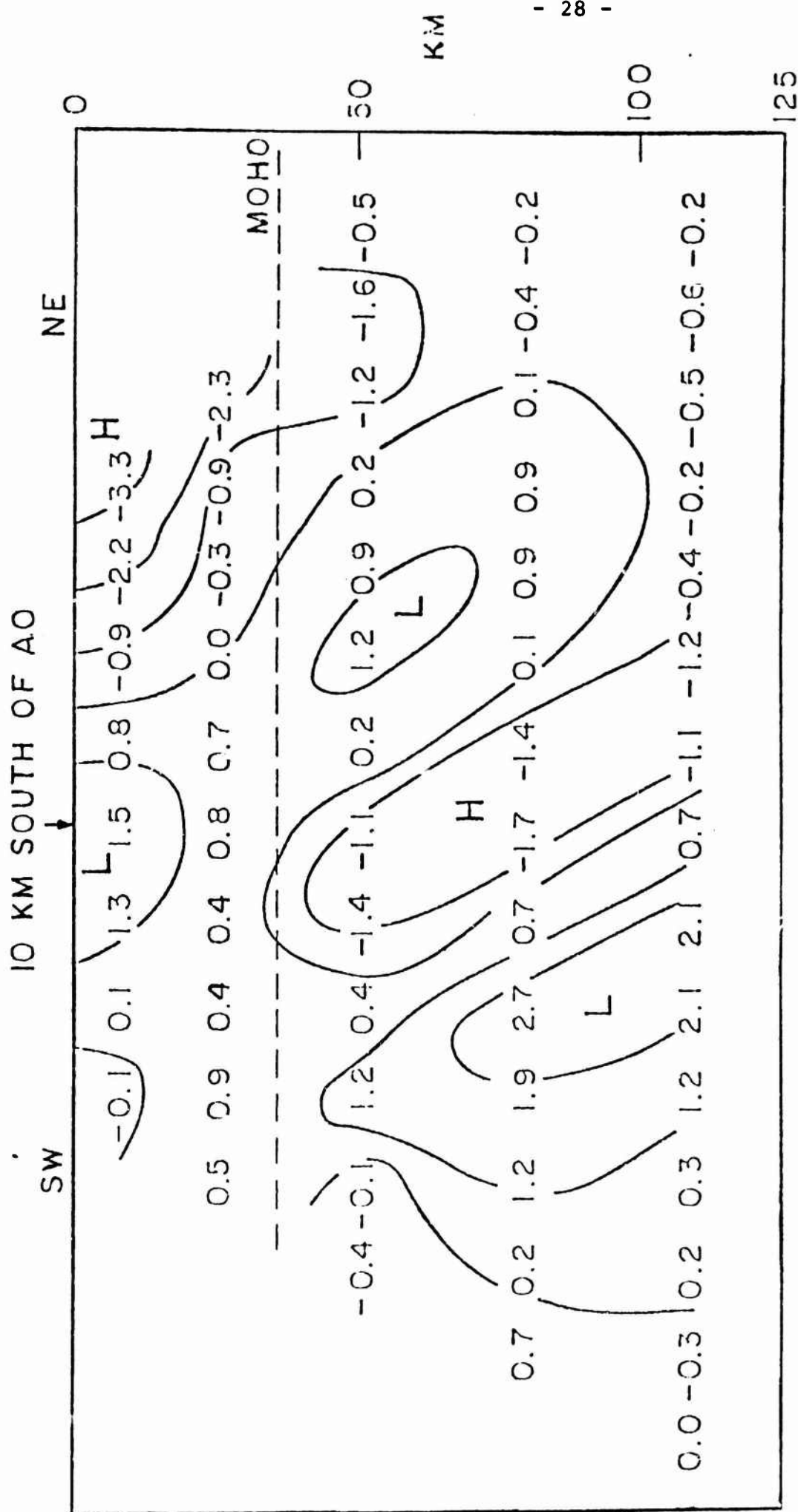
Fig. F.1 A vertical section through the NORSAR area. The values listed are deviations in per cent from average P-velocity. Negative numbers mean high velocity.

G.   UPPER MANTLE P WAVE VELOCITIES

The beam-power processing program described elsewhere in
this report (section A) has been used to estimate apparent
slownesses and azimuths of short period P signals from
some 40 Russian explosions ($12^{O} \leq \Delta \leq 40^{O}$) and a comparable
number of Atlantic earthquakes. Those data which have
sampled only continental paths exhibit consistent evidence
for multibranching in the approx. distance range $15^{O} < \Delta < 28^{O}$.
These data are broadly consistent with a slightly modified
version of the B1 model of Jordan and Anderson (1974). The
observed slownesses and travel times of the explosion data
are plotted in compact form on Fig. G.1 in comparison with
the T-Δ curve entailed by a B1-type model with a modified
velocity gradient in the uppermost mantle and with the
discontinuities near 400 and 650 km reduced in size and
smoothed. A model of this type explains the principal
features of the data (although the need for further refine-
ment and travel-time adjustment is recognized), and equally
important does not entail features blatantly inconsistent
with the data. The notable absence of arrivals corresponding
to the prograde end of the triplication associated with
'the 650 km discontinuity' may be explained by postulating
an increase in Q to accompany the velocity increase at that
depth (see Mereu et al, 1974).

P waves from the North Atlantic earthquakes have upwards
of half of their travel paths in oceanic structures. These
data differ from the continental data insofar as evidence
for multibranching is much less pronounced. The absence of
clear secondary arrivals places some constraint on the size
and nature of possible velocity discontinuities at depth.

Smooth models such as those presented by Kulhanek and Brown (1974) adequately explain most of the observed times and slownesses.

G. Calcagnile and D.W. King

REFERENCES

Jordan, T., and D.L. Anderson (1974): Earth structure from free oscillations and travel times, Geophys. J., 36, 411-459.

Mereu, R.F., D.W. Simpson and D.W. King (1974): Q and its effect on the observation of upper mantle travel-time branches, Earth Planet. Sci. Lett., 21, 439-447.

Kulhanek, O., and R.J. Brown (1974): P wave velocity anomalies in the Earth's mantle from the Uppsala array observations, Pure and Appl. Geophys., 112, 597-617.
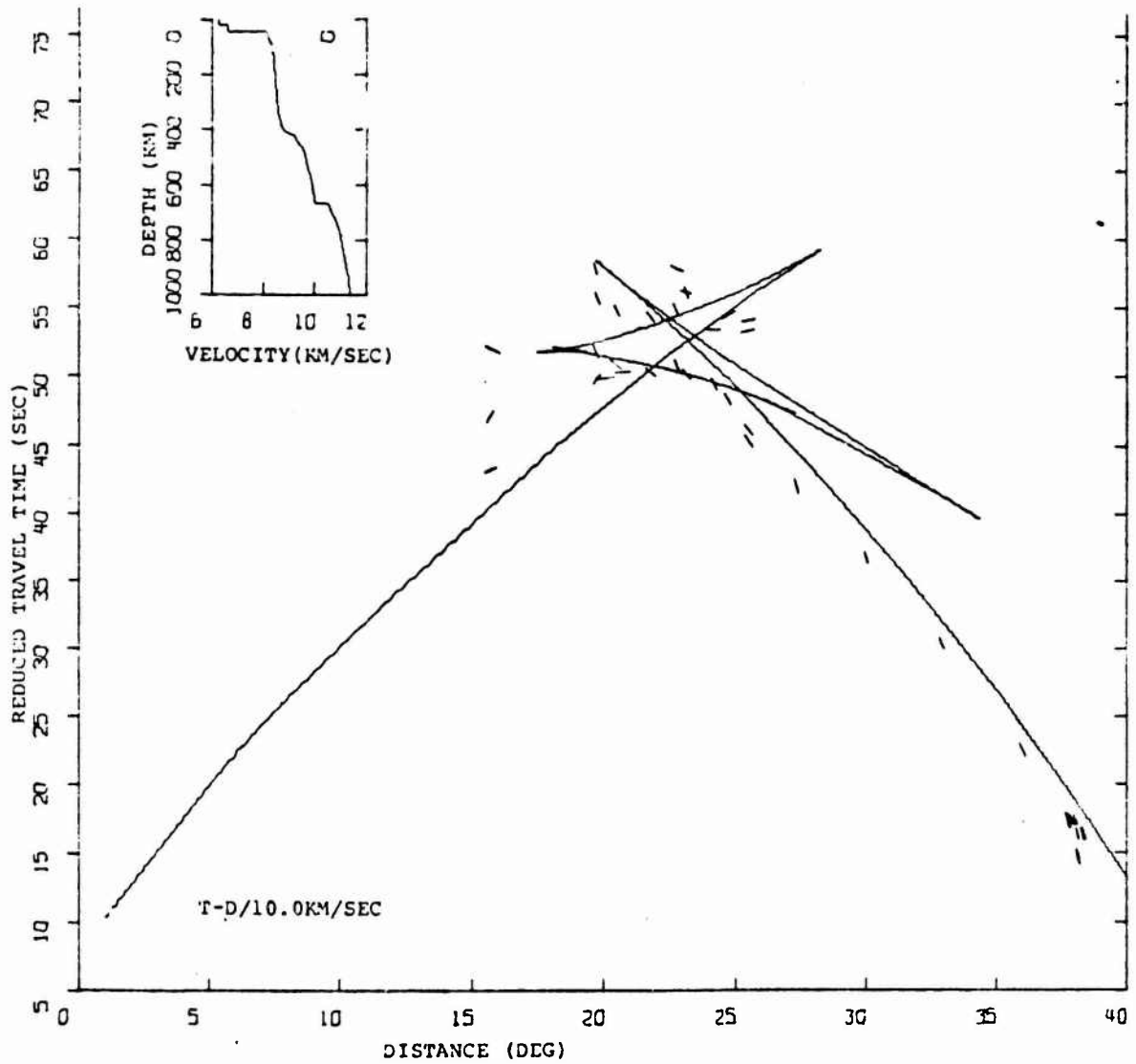
Fig. G.1   Observed slownesses and (reduced) travel times from Russian explosions in comparison with the T-Δ curve entailed by a modified B1 velocity model (inset).

H.   IMPLICATIONS OF CRUSTAL SCATTERING ON SEISMIC PROFILING

There is evidence from numerous disparate sources for the
presence of small-scale random irregularities in the crust
and upper mantle. Estimated characteristic sizes of ir-
regularities are typically in the range from 4.5 meters
(Jeffreys, 1970) to several tens of kilometers (e.g.
Berteussen et al, 1975), but are subject to great uncertain-
ties (Berteussen et al, 1975; King et al, 1975). Notwith-
standing the uncertainties which prevail as to the character-
istic size of the irregularities, their presence would be
expected to scatter relatively strongly the short wave-
length P (and S) waves commonly recorded in seismic profiling
surveys. It is a simple matter to estimate the range of
sizes of irregularities within which the fundamental assump-
tions underlying profiling methods are so seriously violated
that a statistical (diffraction) theory is strictly necessary
in any interpretation. For instance, for a typical signal
wavelength of 2 km and a path length of 300 km, it can be
shown from the acoustic wave scattering theory of Chernov
(1960) that only inhomogeneities smaller than 0.1 km or
greater than 18 kms would permit the application of standard
ray theory.

A number of previous studies have indicated that a significant
part of the irregularities in the vicinity of NORSAR have
characteristic sizes less than about 20 km. It is to be
expected then that recordings of local $(\Delta \lesssim 5^{\circ})$ events should
exhibit features not readily interpretable in terms of ray
theory. A number of local explosions and earthquakes recorded
at NORSAR have been plotted as distance sections and the
durability of various arrivals scrutinized. Almost all ar-
rivals exhibit a great variability over small surface areas.
As an example, data from an earthquake approx. 320 km away

from two subarrays separated laterally by only 40 kms are
plotted on a common section in Fig. H.1. Interpretations of
crustal layering based on subsets of this data would undoubtedly
have grossly different features. This example is by no means
atypical -- records from within 7 km-aperture subarrays
commonly exhibit a comparable variability, particularly
with regard to secondary arrivals. It is planned to re-
examine the uncertainties in crustal interpretations using
the NORSAR recordings from local earthquakes and explosions
distributed widely in azimuth.

D.W. King and K.A. Berteussen

REFERENCES

Berteussen, K.A., A. Christoffersson, E.S. Husebye and A. Dahle (1975):
    Wave scattering theory in analysis of P-wave anomalies at NORSAR
    and LASA, Geophys. J.R. Astr. Soc., in press.

Chernov, L.A. (1960): Wave propagation in a random medium, trans.
    by R.A. Silverman, McGraw-Hill Book Company, New York.

King, D.W., R.A.W. Haddon and E.S. Husebye (1975): Precursors to PP,
    Phys. Earth and Planet. Int., in press.

Jeffreys, H. (1970): The Earth, 5th Ed., Cambridge Univ. Press, New
    York.
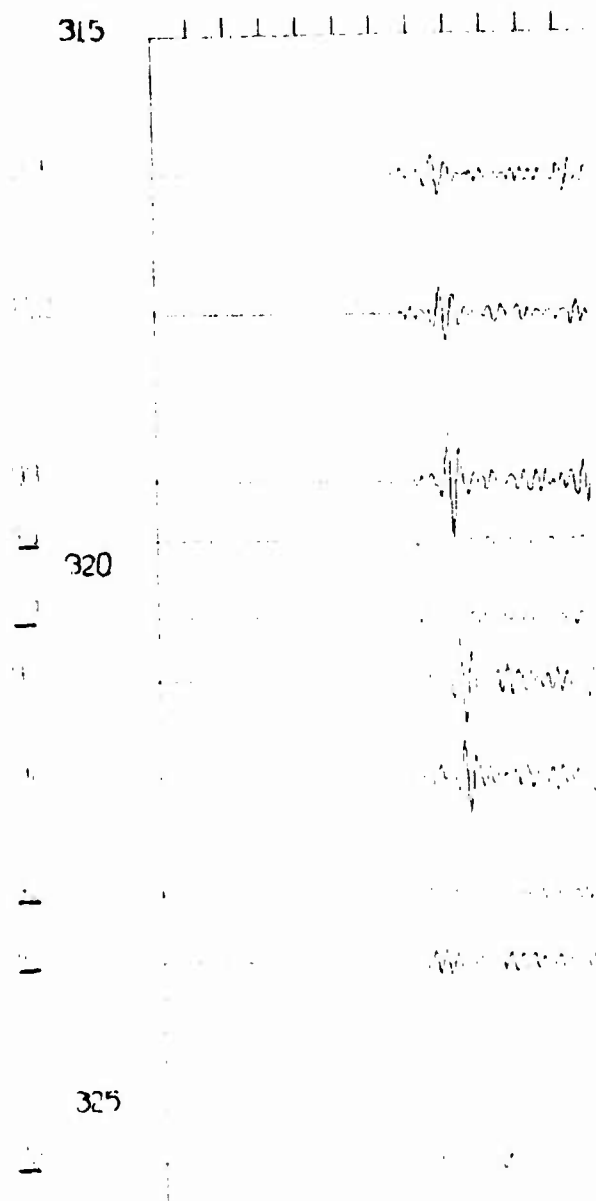
Fig. H.1   NORSAR recorded P-signals for event close to
Haugesund, Norway, 03 April 1975. The leftmost
numbers give instrument number (those underlined
are from subarray 06B while the others are from
subarray 09C). The numbers close to the vertical
axis give kilometer from the source. The distance
between the marks on the horizontal axis is one second.
The data has been filtered with a 1.6-4.4 Hz bandpass
filter.

I. AUTOREGRESSIVE REPRESENTATION OF SEISMIC P-WAVE SIGNALS
    AND SHORT-PERIOD DISCRIMINATION

It is shown that seismic P-wave signals can be represented
by parametric models of autoregressive type. These are
models having the form

$$X(t) - a_1 X(t-1) - \ldots - a_p X(t-p) = Z(t)$$

where $X(t)$ is the digitized short-period data time series
defined by the P-wave signal, and $Z(t)$ is a white noise
series. The autoregressive analysis was undertaken for
40 underground nuclear explosions and 45 earthquakes from
Eurasia. For each event a separate analysis of the noise
preceding the event as well as of the P-wave coda has been
included. It is found that in most cases a reasonable
statistical fit is obtained using a low order autoregressive
model.

The autoregressive parameters characterize the power spectrum
(equivalently, the autocorrelation function) of the P-wave
signal. In fact, for an autoregressive process of order p,
the theoretical power spectrum is given by

$$G(f) = \frac{\sigma_z^2/f_c}{\left| 1-a_1 e^{-\pi i(f/f_c)} - \ldots -a_p e^{-p\pi i(f/f_c)} \right|^2}$$

for $0 \leq f \leq f_c$, where i is the imaginary unit, and $f_c = 1/2h$ is
the cutoff frequency, h being the time interval between
samples. These parameters should form a convenient basis
for studying the possibilities of short-period discrimina-
tion between nuclear explosions and earthquakes, since given
the autoregressive parameters one is able to reconstruct
the power spectrum for the considered event. In principle,
therefore, the study of discriminants using power spectral
properties should reduce to a study of the associated
autoregressive parameters, that is, essentially to a study

of plots such as the one given in Fig. I.1. From this figure and various similar plots we reach the tentative conclusion that it seems difficult to construct really good discriminants based solely on power-spectral properties. However, the autoregressive parameters are of value when combined with other discriminants such as the $m_b:M_s$ criterion (Bungum and Tjøstheim, 1975).

D. Tjøstheim

REFERENCES

Bungum, H., and D. Tjøstheim (1975): Discrimination between Eurasian earthquakes and underground explosions using the $m_b:M_s$ method and short period autoregressive parameters, This report.

Tjøstheim, D. (1975): Autoregressive representation of seismic P-wave signals with an application to the problem of short-period discriminants, Geophys. J. R. Astr. Soc., in press.
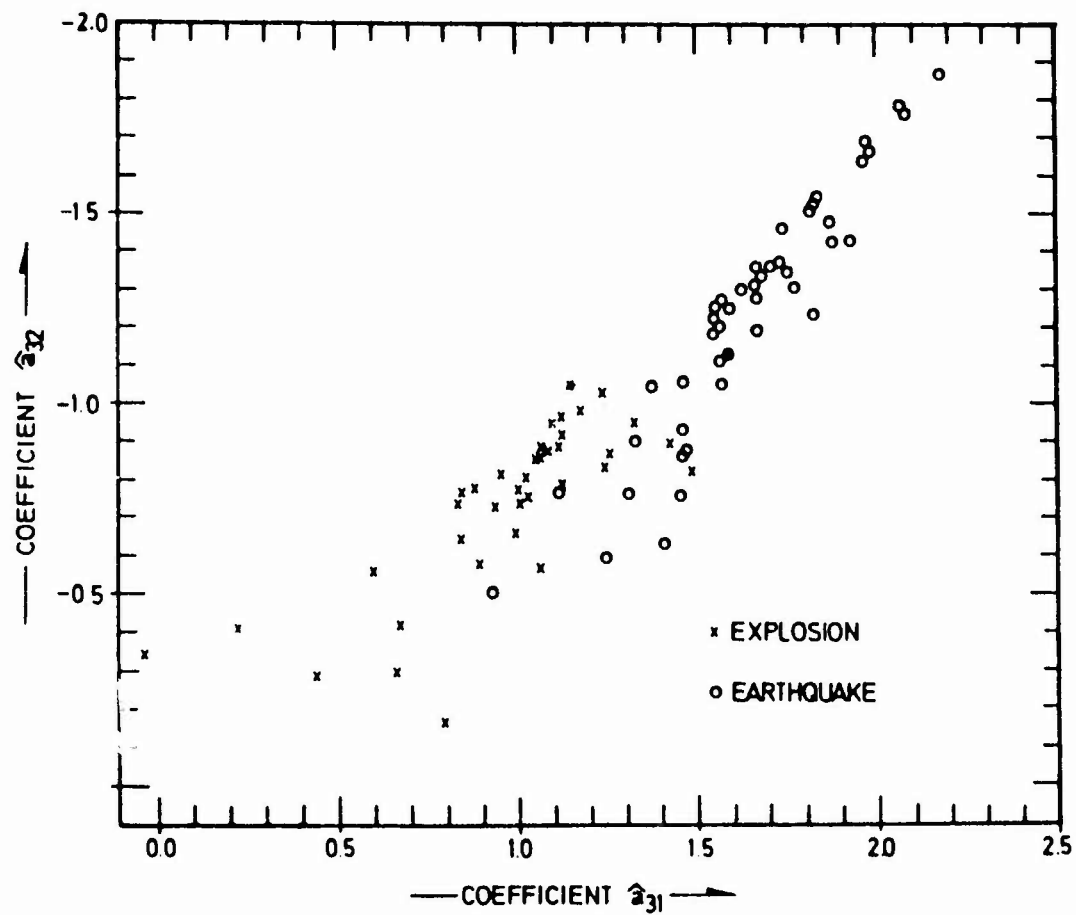
Fig. I.1   Estimated coefficients $\hat{a}_{31}$ and $\hat{a}_{32}$ assuming a 3rd order autoregressive model.

$$X(t) - a_{31} \, X(t-1) - a_{32} \, X(t-2) - a_{33} \, X(t-3) = Z(t).$$

J. SOME AUTOREGRESSIVE MODELS FOR SHORT-PERIOD SEISMIC NOISE

Several investigations have been made into the structure of
seismic noise in general and of the seismic noise at NORSAR
in particular. These studies have been nonparametric in
nature in the sense that they have been concerned with the
general properties of the spectrum and autocorrelation func-
tion of the process. The advantage of having a parametric
model should be obvious. If a good model can be found, the
noise process can be characterized by the numerical values
of a few parameters as opposed to a study of plots of the
spectrum and the autocorrelation function.

It turns out that the short-period seismic noise at NORSAR
can be described by a parametric model having the form

$$X(t) - a_1(t)X(t-1) - \ldots - a_p(t)X(t-p) = Z(t)$$

where $X(t)$ is used to denote the noise process. This is
a nonstationary generalization of the standard autoregressive
models allowing time-varying autoregressive coefficients and
a nonstationary white-noise residual process $Z(t)$. It is
found that the short-period noise at NORSAR is in most cases
quite satisfactorily described by a third order ($p=3$) model.
Also, it is seen from Table J.1 that the nonstationary charac-
ter of the noise is due primarily to time variations of the
residual variance and the lower order autoregressive coef-
ficients.

D. Tjøstheim

REFERENCE

Tjøstheim, D. (1975): Some autoregressive models for short-period
seismic noise, Bull. Seism. Soc. Am., 65, pp. 677-691.

TABLE J.1

Mean, standard deviation and stability parameters of autoregressive coefficients and residual variances for various subarrays. The parameters are obtained by averaging the estimated autoregressive coefficients and residual variances over 34 two-minute noise samples from August 1973. For each two-minute sample a third order autoregressive model has been assumed. The stability parameter gives an indication of the time variations in the model. Low stability means large time variations and vice versa.

Sub-array	$\hat{a}_{31}$			$\hat{a}_{32}$			$\hat{a}_{33}$			$\hat{\sigma}_z^2$		
	Mean	St.Dev.	Stab.	Mean	St.Dev.	Stab.	Mean	St.Dev.	Stab.	Mean	St.Dev.	Stab.
01A	1.68	0.15	11.2	-0.97	0.28	3.5	0.18	0.15	1.2	16323	10584	1.6
01B	1.79	0.13	13.8	-1.01	0.28	3.6	0.15	0.16	0.9	10785	6352	1.7
02B	1.80	0.10	18.0	-1.09	0.20	5.5	0.20	0.10	2.0	9203	4665	2.0
03B	1.63	0.19	8.6	-0.82	0.36	2.3	0.09	0.18	0.5	21438	14072	1.5
05B	1.70	0.17	10.0	-0.95	0.32	2.9	0.14	0.16	0.9	12240	9426	1.3
06B	1.70	0.12	14.2	-0.92	0.22	4.2	0.11	0.12	0.9	10185	6158	1.6
07B	1.73	0.22	7.9	-1.00	0.30	3.3	0.17	0.13	1.3	13402	12839	1.0
01C	1.73	0.10	17.3	-1.00	0.20	5.0	0.18	0.11	1.6	8135	3522	1.3
02C	1.71	0.11	16.5	-0.93	0.28	3.3	0.12	0.15	0.8	9246	5127	1.8
03C	1.64	0.22	7.5	-0.83	0.39	2.1	0.09	0.17	0.5	11633	11273	1.0
04C	1.60	0.19	8.4	-0.74	0.38	1.9	0.04	0.17	0.2	9837	8865	1.1
05C	1.73	0.23	7.5	-0.95	0.37	2.6	0.16	0.17	0.9	10436	8135	1.3
06C	1.72	0.13	13.2	-0.94	0.26	3.6	0.13	0.14	0.9	8457	5656	1.5
07C	1.54	0.18	8.6	-0.68	0.29	2.3	0.02	0.13	0.2	11666	8685	1.3
09C	1.42	0.34	3.9	-0.57	0.47	1.2	-0.00	0.20	0.0	21412	26591	0.8
10C	1.76	0.11	16.0	-1.02	0.17	6.0	0.17	0.10	1.7	10415	6655	1.7
11C	1.72	0.09	19.1	-0.95	0.18	5.3	0.12	0.11	1.1	17061	10639	1.6
12C	1.75	0.13	13.5	-1.00	0.23	4.3	0.14	0.12	1.2	9942	5412	1.8
13C	1.53	0.18	8.4	-0.56	0.25	2.2	-0.08	0.14	0.6	12779	12013	1.0
14C	1.43	0.30	4.8	-0.65	0.35	1.9	0.08	0.14	0.6	23544	8942	2.6

K.   FURTHER $m_b:M_s$ STUDIES AT NORSAR

A comprehensive $m_b:M_s$ analysis has been undertaken using
a data base of 60 presumed nuclear explosions and 45 pre-
sumed earthquakes in Eurasia recorded at NORSAR between
1971 and 1974. The data have been selected subject to the
requirement that both PDE location and magnitude estimates
should be available in addition to the recordings at NORSAR.
The geographic distribution of these events is given in
Fig. K.1; notice that 35 of the presumed explosions are con-
fined to a small area in Eastern Kazakh.

The $m_b:M_s$ relationship was investigated using both NORSAR
and PDE estimates for the body wave magnitude m_b. It was
found that while m_b(NORSAR) gave a slightly better
separation for the Eastern Kazakh data (see Fig. K.1),
m_b(PDE) gave significantly better results when applied
to the complete data set, this being due to a magnitude
bias caused by a larger power loss in array beamforming for
events with smaller travel distance ($<30^o$).

The basic results of this $m_b:M_s$ analysis are given in
Fig. K.2, where m_b(PDE) is plotted versus M_s(NORSAR). It
was possible to estimate M_s for 44 of the presumed explo-
sions, for the other 16 an upper bound is given, determined
by the noise level at that particular time. Among the 44
explosions there are 3 difficult events, all on the edge
of the earthquake population. Two of those are from the
Ural Mountains (March 22, 1971, and October 26, 1973),
while the smallest and most difficult one to identify is
from Novaya Zemlya (July 22, 1974). Several of the events
for which no Rayleigh waves have been identified occurred
during a period when the noise level was low enough to
allow identification based on negative evidence, while others
are falling between the two populations.
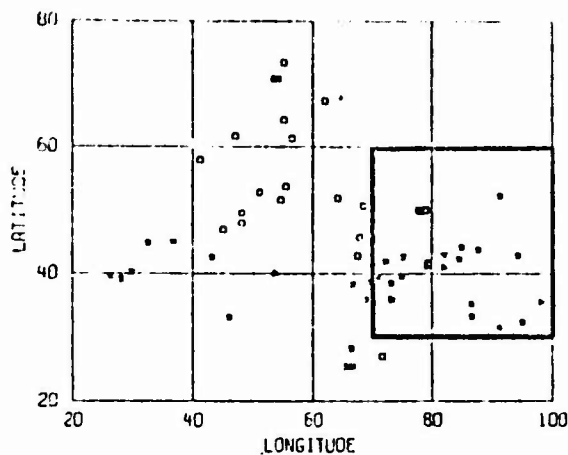
Fig. K.1   The geographic distribution of the 60 explosions and 45
            earthquakes used in this study. Explosions are depicted
            by squares and earthquakes by stars. The area between
            $30^\circ - 60^\circ$N and $70^\circ - 100^\circ$E is that called 'Eastern Kazakh'.
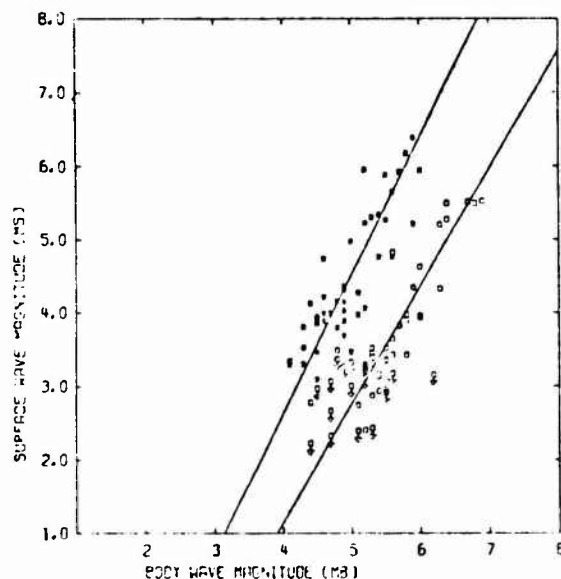
Fig. K.2 $m_b:M_s$ diagram for the complete data base of 60 explosions
            and 45 earthquakes from Eurasia, including 16 explosions for
            which no Rayleigh waves have been detected at NORSAR. The
            symbol for each of these 16 events includes an arrow to
            indicate that the M_s value has been replaced by a noise
            estimate representing the largest possible M_s value.

In order to evaluate numerically the separation in Fig. K.2, a discriminant was defined which is a linear combination of m_b and M_s such that it is zero everywhere on the explosion regression line. From the distributions of the explosion and earthquake discriminant values the identification probability can be estimated for any particular false alarm rate. It was found for the data in Fig. K.2 that for a false alarm rate of 1% one would have an identification probability of 90.3%. Furthermore, if the 16 explosions with no Rayleigh waves detected were removed, the identification probability would increase to 95.4%, still for a false alarm rate of 1%.

The 16 noise measurements in Fig. K.2 are distributed almost randomly in time over about 4 years. The average value, which is M_s=2.9, can therefore be used as a measure of the detectability level for explosion Rayleigh waves from Eurasia, and the standard deviation is estimated to $\pm$ 0.4 M_s units. This large standard deviation is caused by large long term fluctuations in the noise level, and in order to investigate that effect more thoroughly, the on-line system at NORSAR was extended to allow for calculation of the average long period noise level. One year of such analysis is shown in Fig. K.3, and a separate calculation of the distribution shows that 70% of the time the variation is within $\pm$8 dB of the median. Provided that there is an inverse linear relationship between noise level and detectability this corresponds to a standard deviation of about $\pm$0.4 M_s units in detectability, which is equal to the value we estimated using the direct method.

H. Bungum
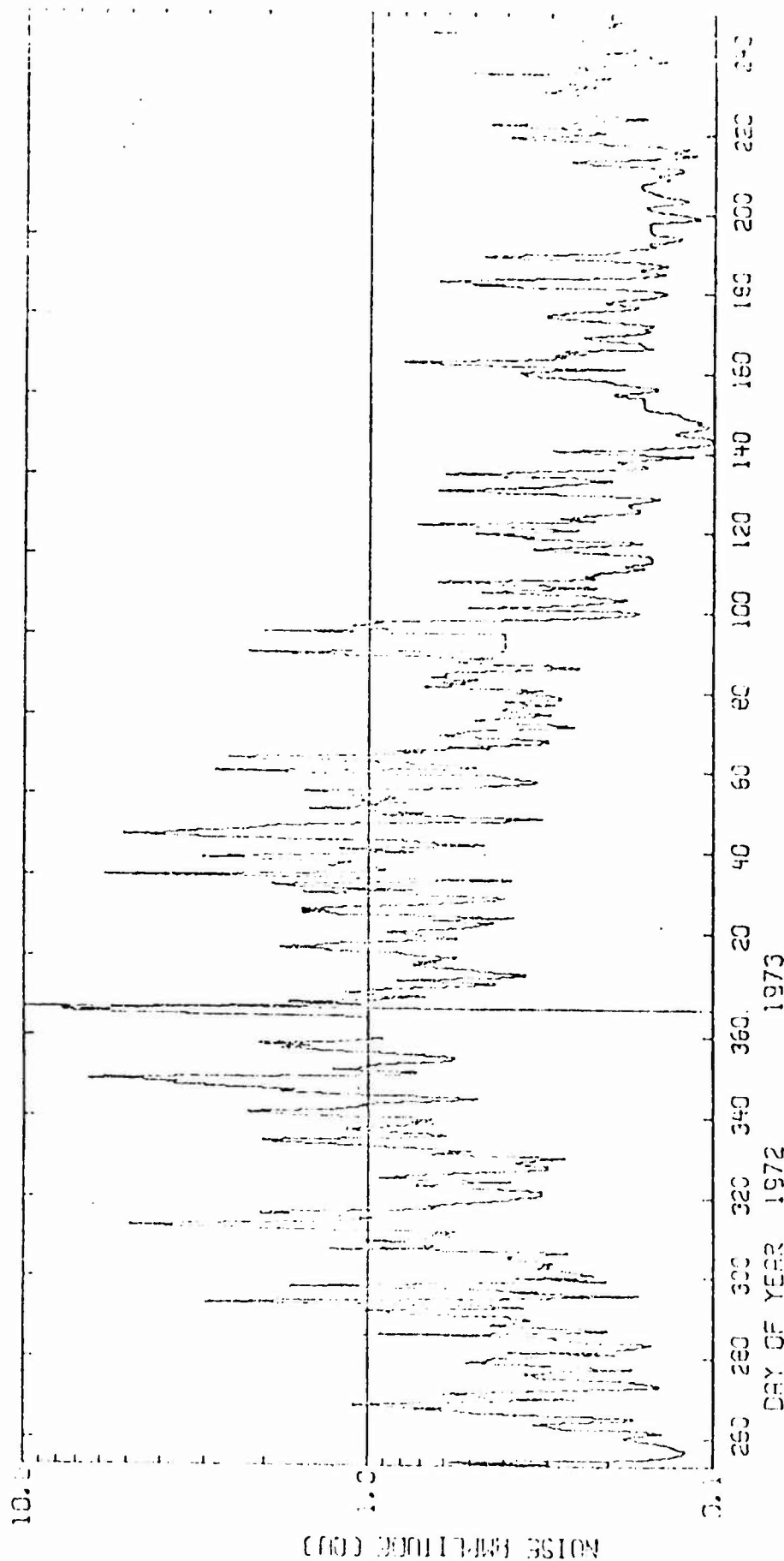
Fig. K.3 Average long period noise level at NORSAR for one year from day 253/72 to day 252/73. The data are actually the average of the noise levels at 14 vertical long period seismometers, where, for each noise sample the highest four and lowest four of the 22 subarrays have been excluded for reasons of stability. The amplitudes are given in arbitrary units, and the sampling rate is 20 per day.

L.   IMPROVED IDENTIFICATION USING COMBINED CRITERIA

In Section K a relatively large data base was presented
in an m_b:M_s analysis of seismic events from Eurasia. The
same data base will be used in this section, only that we
have proceeded one step further and combined the m_b:M_s data
with more short period information in order to further
improve the separation between earthquakes and explosions.
Such combinations are often done through successive applica-
tion of discriminants, starting with the best one. Combining
discriminants linearly, however, results in several advantages.
First of all, the same analysis applies to all events so that
the analyst can enter with his interpretation at a higher
level; secondly, a combined discriminant is easier to
evaluate than a step-wise procedure. In this study we have
defined a new two-dimensional discriminant which in many
ways can be compared with the m_b:M_s discriminant.

The new discriminant is constructed by combining the m_b:M_s
data with some parameters obtained by modelling the short
period data, noise as well as main signal and coda, as auto-
regressive time series. For more details we refer to
Tjøstheim (1975); see also Section I, where it was found
that such modelling is in fact possible, and in most cases
a good approximation is obtained using a third order
model. The three resulting coefficients then essentially
describe the second order structure or the power spectrum
of the particular time series under consideration.

The optimal linear combinations have been obtained through
an extensive trial-and-error procedure, where a large number
of combinations have been tested. The best one was obtained
by defining the two parameters of the new discriminant as

$$X1 = m_b - B \cdot \hat{a}_1(S)$$
$$X2 = M_s + B \cdot (\hat{a}_1(C) - \hat{a}_1(N)) \tag{L.1}$$

where $\hat{a}_1(S)$ is the first order coefficient from the main
signal, and C and N denote coda and preceding noise respectively.
It was reassuring to note that the above discriminant
gave the best results even when applied to different data
bases and different regions (in Eurasia, that is), and the
same kind of stability was observed for the scaling coeffi-
cient B, whose optimal value usually was found to be around
0.5.

An example of the new two-dimensional discriminant as applied
to data from around Eastern Kazakh is given in Figs. L.1
and L.2, where the $m_b:M_s$ and the corresponding X1:X2 diagrams
are given respectively. It is easily seen that the improve-
ment in separation is considerable.

H. Bungum and D. Tjøstheim

REFERENCES

Tjøstheim, D. (1975): Autoregressive representation of seismic P-wave
    signals with an application to the problem of short-period
    discriminants, Geophys. J.R. Astr. Soc., in press.

Fig. L.2

X1:X2 diagram for the same data as in Fig. L.1, using formula (L.1) with B 0.5.

Fig. L.1

$M_b:M_s$ diagram for the 'Eastern Kazakh' data base of explosions and 31 earthquakes.

M. A KIRNOS SEISMOGRAPH IN THE NORSAR SEISMIC ARRAY

The differences in earthquake magnitudes measured from wide
band (Kirnos) seismographs, such as are widely installed in
the USSR ('East and narrow band seismographs used in
'Western' installations have been discussed at great lengths
in the Geneva test ban negotiations (CCD). The displacement
response for the two instrument types are shown in Fig. M.1.
Operation of Hall-Sears (U.S.A.) and Kirnos (U.S.S.R.) seis-
mometers at the same site suggests itself as a useful
experiment directed to clarifying the discrepancies between
'Eastern' and 'Western' body wave magnitudes.
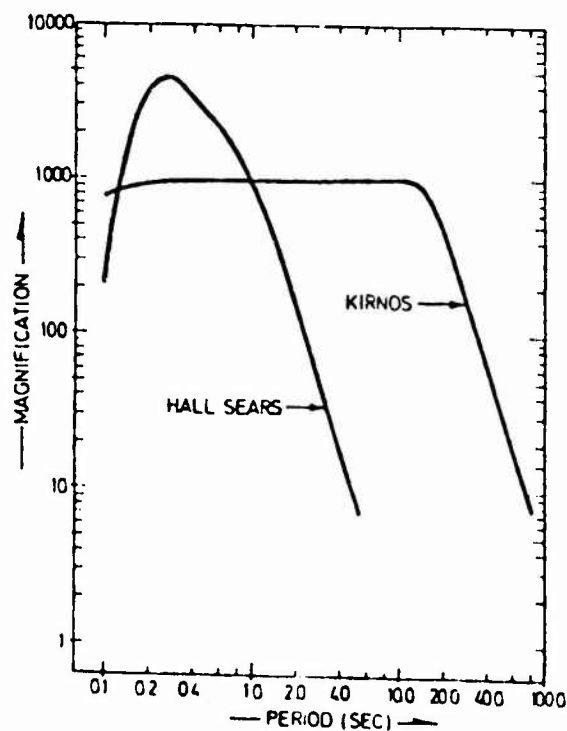
Fig. M.1   Displacement response for Kirnos SVK-2 compared to the
NORSAR seismometer response (Hall-Sears). Equal magni-
fication at 1 sec period.

As a part of a Nordic project on detection seismology,
a Kirnos vertical broadband instrument was installed at
NORSAR subarray 04B and operated over a period of about nine
months. During the period of operation (Jan-Sep 1974) the
seismograms from the Kirnos instrumentation have been read
in comparison with the NORSAR bulletin. On an average some
twelve events have been identified every month, with more
events detected in summer than in winter. Fig. M.2 shows
the decision histogram together with the maximum likelihood
estimated thresholds of 5.7 and 6.4 body wave magnitude
for 50 and 90 per cent probability of detection, respectively.
All wave modes are included in the detection decision in
this case. When only body waves (P, PP, PcP, PKP) are con-
sidered, the results are even more modest for the Kirnos
seismograph detectability, namely, 5.9 and 6.5 m_b units.
However, it has to be pointed out that the reliability of
the estimates decreases when sample size is significantly
less than one hundred.

Due to poor detectability, the Kirnos seismograph system
would need years of operation in Norway in order to establish
a reasonable data base suitable for statistical magnitude
studies. However, it might be interesting to see if the
limited data available follow the general trend that would
be expected from a broadband instrument of the SVK-2 type.
Due to the paucity of observations, no regionalization was
attempted, and, moreover, core phases are excluded from the
magnitude considerations in the following. Altogether 25 events
in the distance range 18-91 degrees were jointly recorded
as P-waves by the Kirnos and the NORSAR Hall-Sears instru-
ment at subarray site 04B00, the two instruments being
separated physically by only 2 meters. The body wave magni-
tude m_b^E computed by the 'Eastern' broadband instrument versus
m_b^W computed by the 'Western' SP instrument is shown in Fig.
M.3. According to Davies (1968), the difference $m_b^E - m_b^W$ should
be around 0.5 magnitude units, while Marshall et al (1972)
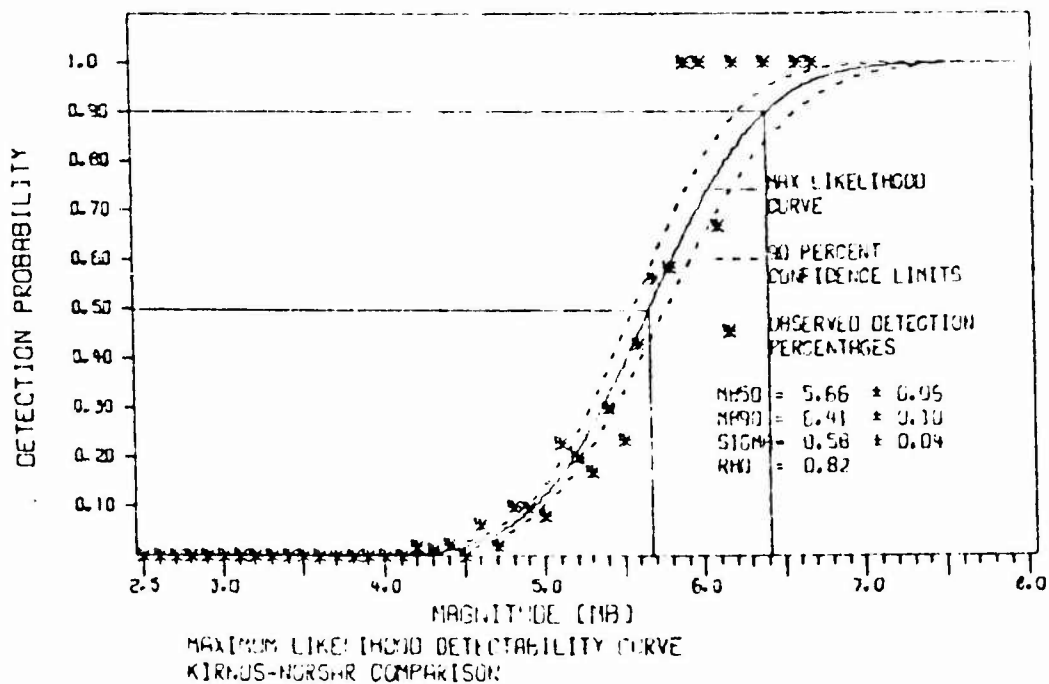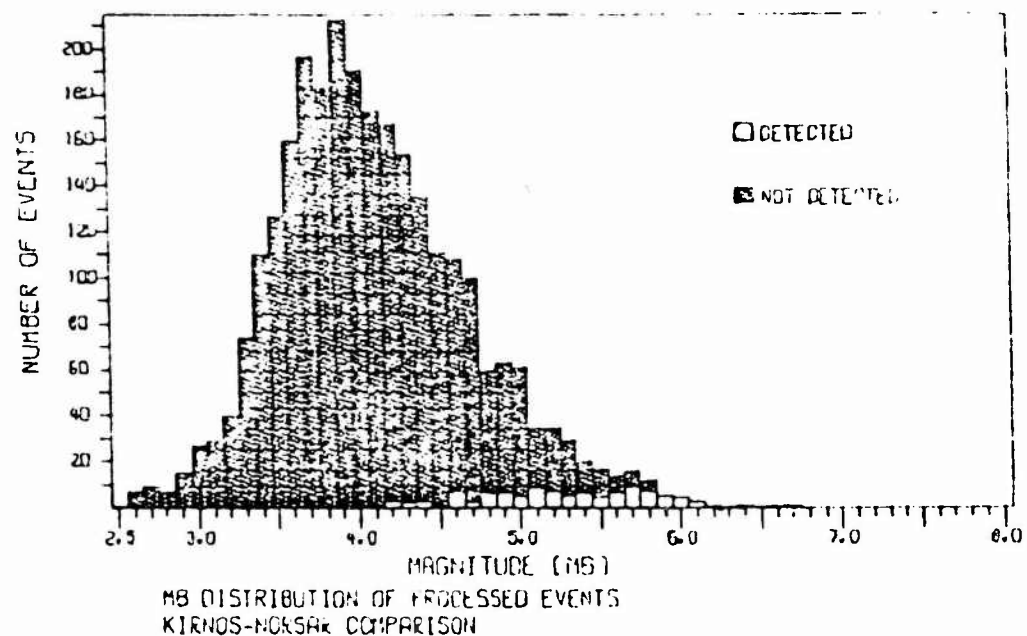
Fig. M.2   Kirnos detection statistics for the total number of events identified (all phases included).
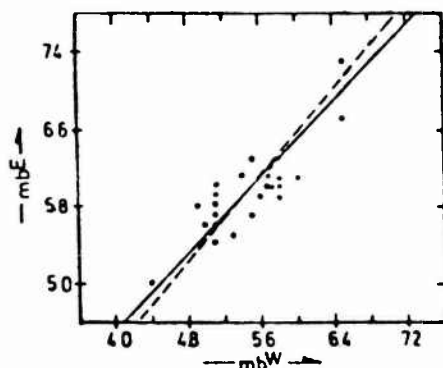
Fig. M.3   Kirnos m_b^E versus Hall-Sears m_b^W. Dotted line: 'Eastern'-
'Western' magnitude relationship by Marshall et al (1972).
Solid line: E-W magnitude relationship by Davies (1968).

found this relationship to be magnitude dependent, yielding

$$m_b^E = 1.12\ m_b^W - 0.15$$

Both these curves are given in Fig. M.3, and the data is not
inconsistent with either.

The results obtained in this study support the conclusion
that the main cause of the discrepancy between 'Eastern'
and 'Western' measurements of magnitude is the difference
in frequency responses of the seismographs employed. A rough
estimate of the slope b of the frequency-magnitude relation-
ship for the Kirnos gives a much lower value than reported
for 'Western' narrowband instrumentation (Richter, 1958;
Marshall et al, 1972). Thus by extrapolation, 'Western'
data predicts more small shocks and fewer great shocks than
'Eastern' broadband data collected by Kirnos instruments.
The Kirnos event detectability is poor, as the noise level
imposes a serious limitation on this broadband system. In

conclusion, it should be stressed that in the present con-
text a minimum requirement for a useful broadband seismograph
system should include magnetic tape recording to permit such
operations as frequency filtering.

More details from this project are to be found in the
report of Dahle (1975).

A. Dahle

REFERENCES

Dahle, A. (1975): A Kirnos seismograph in the NORSAR Seismic Array,
Internal Report No. 4-74/75, NTNF/NORSAR, Kjeller, Norway.

Davies, D. (1968): Seismic methods for monitoring underground explo-
sions, Almquist & Wiksell, Sweden.

Marshall, P.D., R.F. Burch and A. Douglas (1972): How and why to
record broadband seismic signals, Nature, 239, No. 5368, 154-155.

Richter, C.F. (1958): Elementary Seismology, W.H. Freeman & Company,
San Francisco and London.

N.   SIGNAL-NOISE CLASSIFICATION

When an event has triggered the NORSAR automatic event
detector, the analyst is faced with the problem of deciding
whether this is earthquake- or explosion-generated seismic
signals or just correlated noise. His data are the seismo-
grams from the 22 subarrays, filtered and time-shifted
according to the estimated epicenter, and the array beam,
the phased sum of the sensors, which has a signal-to-noise
ratio about 13 dB better than the individual subarrays.
Together with this he uses his experience about the
signal shape, the subarray amplitude distribution, detecta-
bility and seismicity in the actual area. In most cases the
signal-to-noise ratios on the subarray level are high
enough to see the incoming P-wave on all or some of the
subarrays, and the decision is easily made. But when the
signal-to-noise ratio is so low that only the beam and
maybe a few subarrays have a visual signal, then the analyst
must use other information as a basis for a decision.
As an aid to the analyst, three different statistical
tests were implemented in the Event Processor in December
1974 to test the hypothesis whether the triggering wavelet
is correlated noise or a real seismic signal. The test
statistics are calculated for events with signal-to-noise
ratios in an interval just above the (time-varying) pre-
threshold. One test statistic considered is the Sign-bit
Semblance test which checks on the signal similarity between
subarrays. Another is a Binomial test which checks on the
sign distribution of least square amplitude weights cal-
culated for the subarray beam traces. The third test sta-
tistic is a Student's t-test which checks on the distribution
and size of subarray beam amplitude weights.

The amplitude weights are an estimate of the amplitude factor, γ_j, in the model $Y_j = \gamma_j S + n_j$, where Y_j is the recorded data on the j-th sensor, S a signal part and n_j a noise part (Fyen et al, 1975). For noise wavelets, the amplitude weights will be random in sign and size, while for P-waves the $\hat{\gamma}_j$-weights are expected to match the amplitude pattern in the region in question. However, for events with a signal-to-noise ratio as small as 3.6-4.0 units, the $\hat{\gamma}$-weights contain reliable amplitude information for the "best" subarrays only, and the correspondence between the observed $\hat{\gamma}_j$-weights and the known amplitude pattern for larger earthquakes is small, a problem which will be investigated further. Also for some extreme cases, noise has the same characteristics as an earthquake signal, as seen in Fig. N.1 where the test statistics accepted the event, but these cases may be eliminated by the anlyst due to his experience of earthquake occurrence and signal shape.

Another type of events which give test statistics results high above the thresholds are events with magnitudes below 4.0 located on the west coast of America and mid-Atlantic Ridge, where NORSAR normally only detects earthquakes above magnitude 4.6. These events are correctly classified by the analyst as being correlated noise and represent most of the statistical false alarms. For events having their origin to the east of NORSAR, we did a case study of weak Japan events. A list of events located in the Japan area, including both cases classified as noise and cases classified as earthquakes, was sent to Japan Meteorological Agency (JMA). Out of 36 events listed, 20 NORSAR-reported earthquakes were confirmed by JMA-stations, and 5 of these earthquakes were classified as noise by the test statistics (missed detections). Out of the remaining 16 events, 11 were not reported in the NORSAR bulletin, nor reported by any JMA-station, and 4 of these were classified as signals by test statistics (false alarms). The 5 other events were out of range for the JMA-stations. After 5 months of processing experience there has been no significant increase in the number of earthquakes

01A 249	0.027
01B 277	0.574
02B 187	-0.012
03B 262	-0.061
04B 295	0.109
05B 237	-0.0
06B 177	-0.036
07B 224	0.040
01C 139	0.005
02C 224	0.379
03C 173	0.234
04C 223	0.121
05C 246	0.371
06C 206	0.035
07C 180	0.273
08C 265	0.184
09C 249	0.347
10C 215	0.246
11C 279	0.239
12C 230	0.264
13C 170	0.030
14C 196	0.098
2A 1494	SNR=4.0
3B 571	SNR=5.1
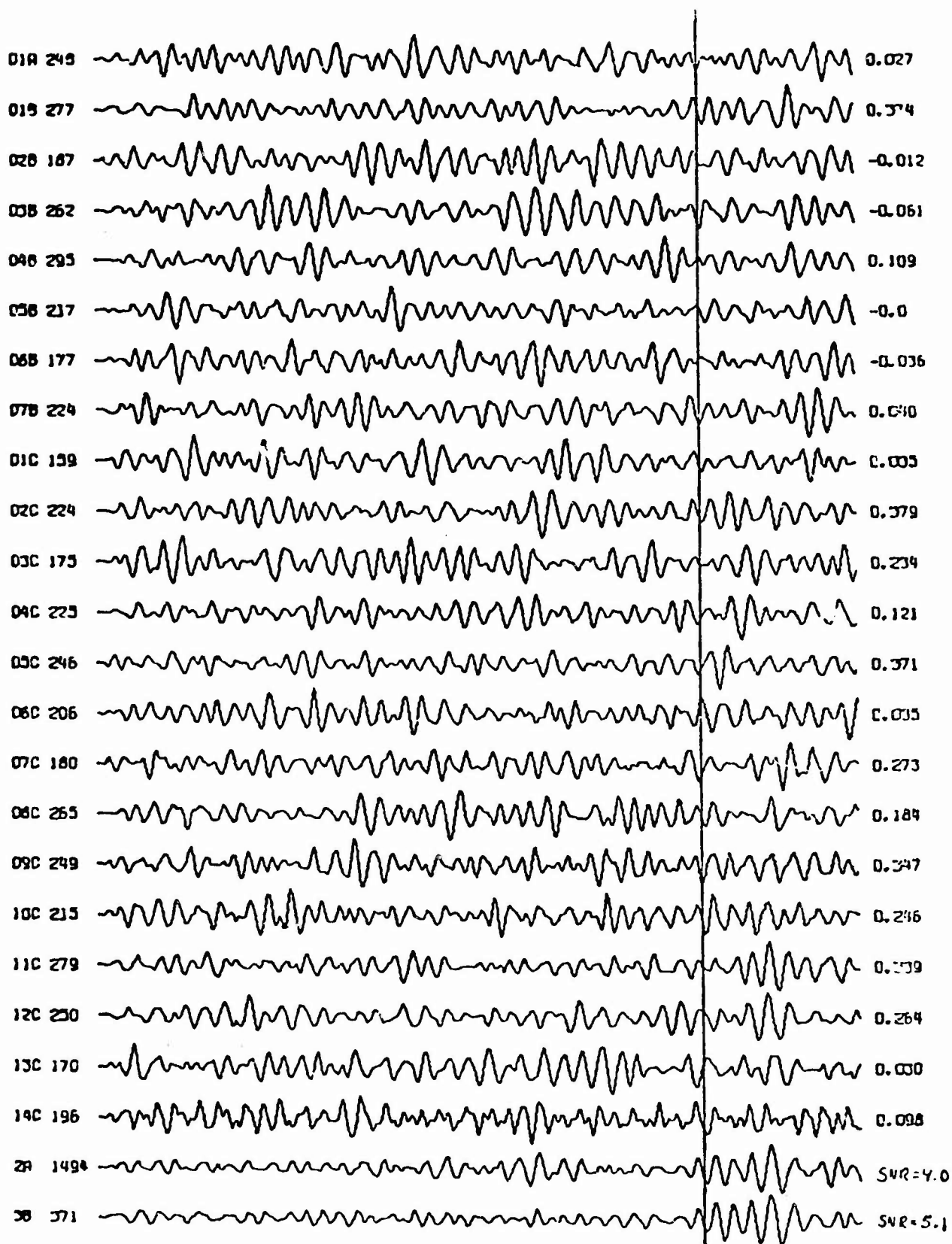
Fig. N.1 Example of extreme noise wavelets. The column to the right gives the $\hat{\gamma}_j$-weights. 2A and 3B denote array and weighted array beam respectively, pointing south of Honshu, Japan. The test results give high signal similarity and non-random sign and size of the amplitude weights, but a check with the amplitude pattern rejects this event as being an earthquake in Japan area.

reported by the analyst due to the test statistics. However, the tests are still considered as a good aid for the marginal cases, and also help the analyst to check whether the line-up of the subarray traces is good, i.e., giving correct time-delays for epicenter determination.

J. Fyen

REFERENCES

Fyen, J. E.S. Husebye and A. Christoffersson (1975): Statistical classification of weak seismic signals and noise at the NORSAR array, Geophys. J.R. Astr. Soc., 42, in press.

O.   PRELIMINARY RAYLEIGH WAVE STUDIES NORTH OF SCANDINAVIA

Surface wave dispersion measurements taken to periods of
the order of 100 sec or more have proved to be diagnostic
of the properties of the upper mantle to depths of the order
of about 0.5 λm for Rayleigh waves, where λm is the longest
wave length.

The results obtained from great-circle passages are not
representative of any particular ocean, shield or tectonic
province. Instead they represent the averages of a variety
of each of the three types of structural provinces
(Dziewonski, 1971). Knopoff (1972) has described in detail
the advantages of pure-path regional studies compared with
"great circle decomposition" methods.

To overcome the difficulties of determining the initial phase
of the source which is encountered in the single-station
phase velocity measurements (Knopoff and Schwab, 1968)
the two-station method is used. Under the assumption that
the angle between the great-circle path between the earth-
quake and the stations on the one hand and the great-circle
connecting the stations on the other hand is small (less
than about 7°), the effect of the initial phase of the source
is eliminated. The two-station method was first used by
Brune and Dorman (1963) with peak-and-trough analysis and
subsequently with machine Fourier analysis by Knopoff,
Mueller and Pilout (1966).

To obtain phase velocities, the seismograms and the instru-
ment responses of each station are digitized at a fixed
interval of 2 sec, an interval sufficiently short to avoid
aliasing problems for this study. The technique of Pilout
and Knopoff (1964) and Knopoff et al (1966) for bandpass,
digital filtering of detrended, digitized seismograms was
applied to minimize the interference effects of multipath
transmission. This procedure significantly improves the
signal-to-noise ratio for complex records. The numerical window

centered at the group arrival time is in the form of a half
cycle of a sine function. Fourier analysis of each of the
filtered seismograms gives the phases in the frequency
band of the numerical filters. In Fig. 0.1 an example is
shown of the raw, filtered, and filtered-windowed time
series.

For two stations on the same great-circle and recording the
same event, the phase velocity at a given period T is given
by

$$C(T) = \frac{D_2-D_1}{T[N+(\phi_2-\phi_1)]}$$

where D_2-D_1 is the station separation, $\phi_2-\phi_1$ is the difference
in the phase shifts (in circle) between the two recordings,
taking into account instrumental phase shifts; the arbitrary
integer N is determined by making the phase velocity geo-
physically suitable at long periods and extending the phase
continuously into the short period regime.

It should be noted that a systematic bias exists in the
Love wave observations due to interference between funda-
mental and I higher mode in the range 30-90 secs. For this
reason Rayleigh waves are more convenient for this type of
study. Fundamental Rayleigh wave phase velocities were ob-
tained with the previous technique for the path KBS-KRK
shown in Fig. 0.2, analyzing the event occurring at 06:26:15.8
the 28th of December 1967.

Unusually high values were found (Fig. 0.3). They are com-
pared with the values obtained by Noponen (1966) in Finland.
The agreement between the two sets of data is good and we
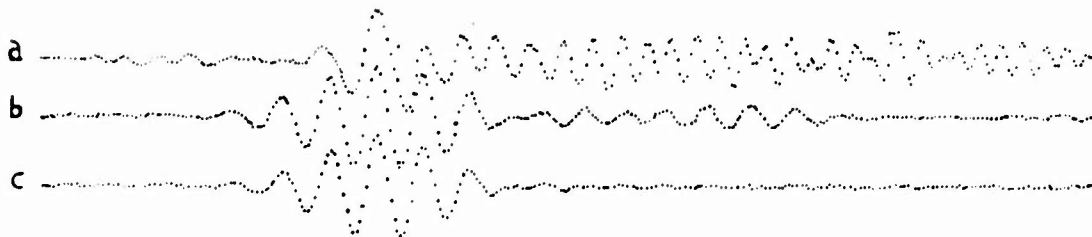
PASS BAND 25·35 sec

Fig. O.1   Example of raw, filtered and filtered-windowed time series.
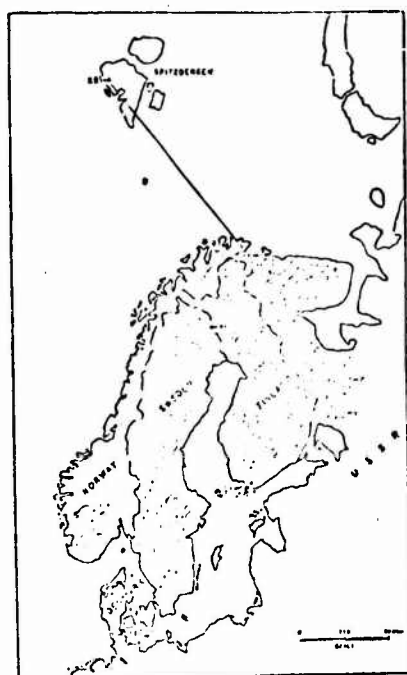
Fig. O.2   Baltic shield and profile considered in this study.
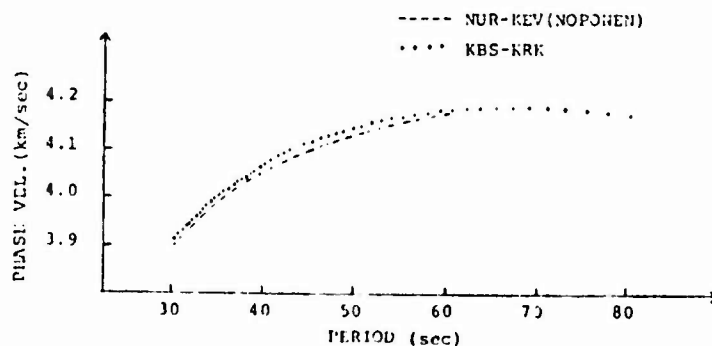
Fig. O.3   Rayleigh wave phase velocity vs. period
            experimental : dots
            NUR-KEV (Noponen) : dashed line

may infer that the uppermost mantle is similar in the two regions.

Work is now in progress aimed at a more detailed interpretation of the experimental data.

G. Calcagnile

REFERENCES

Brune, J., and J. Dorman (1963): Seismic waves and earth structure in the Canadian shield, Bull. Seism. Soc. Am., 53, 167-210.

Dziewonski, A. (1971): Upper mantle models from "pure-path" dispersion data, J. Geophys. Res., 76, 2587-2601.

Knopoff, L. (1972): Observation and inversion of surface-wave dispersion, The Upper Mantle, ed. A.R. Ritsema, Elsevier Publ. Co., Amsterdam, Tectonophysics, 13, 497-519.

Knopoff, L., S. Mueller and W.L. Pilout (1966): Structure of the crust and upper mantle in the Alps from the phase velocity of Rayleigh waves, Bull. Seism. Soc. Am., 56, 1009-1044.

Knopoff, L., and F.A. Schwab (1968): Apparent initial phase of a source of Rayleigh waves, J. Geophys. Res., 73, 755-760.

Noponen, I. (1966): Surface wave phase velocities in Finland, Bull. Seism. Soc. Am., 56, 1093-1104.

Pilout, W.L. and L. Knopoff (1964): Observations of multiple seismic events, Bull. Seism. Soc. Am., 54, 19-39.

P. HIGHER MODE SURFACE WAVES

Higher mode surface waves are valuable for probing the struc-
ture of the uppermost mantle on account of their selective
depth sampling. Attempts to exploit higher modes are generally
frustrated by the necessity for long, homogeneous paths and
by limitations in the dynamic range of most recording devices.
However, NORSAR's siting and digital recording is such that
higher modes are commonly well-recorded from sources in
Sinkiang, Central Russia, Southern Europe and Novaya Zemlya.

It has been suggested previously (Crampin, 1966) that higher
mode propagation over much of Eurasia exhibits mode coupling
which apparently finds no satisfactory explanation in isotropic
Earth models. Crampin (1967) suggested an interpretation
involving a thin layer of aligned crystalline anisotropy
in the uppermost mantle, and has subsequently explored
theoretically the implications of such an interpretation
(Crampin, 1970; Crampin and Taylor, 1971; Crampin, 1975).
The principal features include distinctive particle motion,
differences in phase (wave) and group direction, and the
generation of Love waves by atmospheric explosions.

NORSAR is potentially (and perhaps uniquely) suitable for a
detailed examination of higher mode propagation in Eurasia;
the spatial sampling of the NORSAR configuration offers the
possibility of multiple analyses of particle motion as well
as of direct estimation of phase and group direction. A
data base of some 14 events with well-recorded higher mode
wave trains has been assembled and representative examples
from 2 events are plotted in Fig. P.1. These data commonly
exhibit mode coupling between vertical and horizontal trans-
verse components over extended sections of the higher mode
trains. Phase velocities and directions of higher mode and
fundamental mode arrivals are being estimated using high-
resolution f-k analysis, and have revealed significant

($\sim 10^{\circ}$) differences in phase direction between the two wave groups along some paths (e.g., Sinkiang). Attempts to measure group velocity and direction of fundamental mode waves by fitting a least squares wavefront to interpolated peaks of envelopes formed from narrow band Gaussian filtered data have yielded encouraging results and may provide determinations sufficiently reliable for comparison with phase determinations.

Finally, NORSAR recorded Love waves of peak amplitude only slightly less than the Rayleigh waves from a large atmospheric explosion in southern Sinkiang in June, 1974. The possibility of explaining this observation in terms of mode conversion after propagation in an anisotropic region is being explored.

D.W. King and S. Crampin

REFERENCES

Crampin, S. (1966): Higher modes of seismic surface wave: Propagation in Eurasia, Bull. Seism. Soc. Am., 56, 1227-1239.

Crampin, S. (1967): Coupled Rayleigh-Love second modes, Geophys. J., 12, 229-235.

Crampin, S. (1970): The dispersion of surface waves in multilayered anisotropic media, Geophys. J., 21, 387-402.

Crampin, S., and D.B. Taylor (1971): The propagation of surface waves in anisotropic media, Geophys. J., 25, 71-87.

Crampin, S. (1975): Distinctive particle motion of surface waves in anisotropic media, Geophys. J., 40, 177-186.
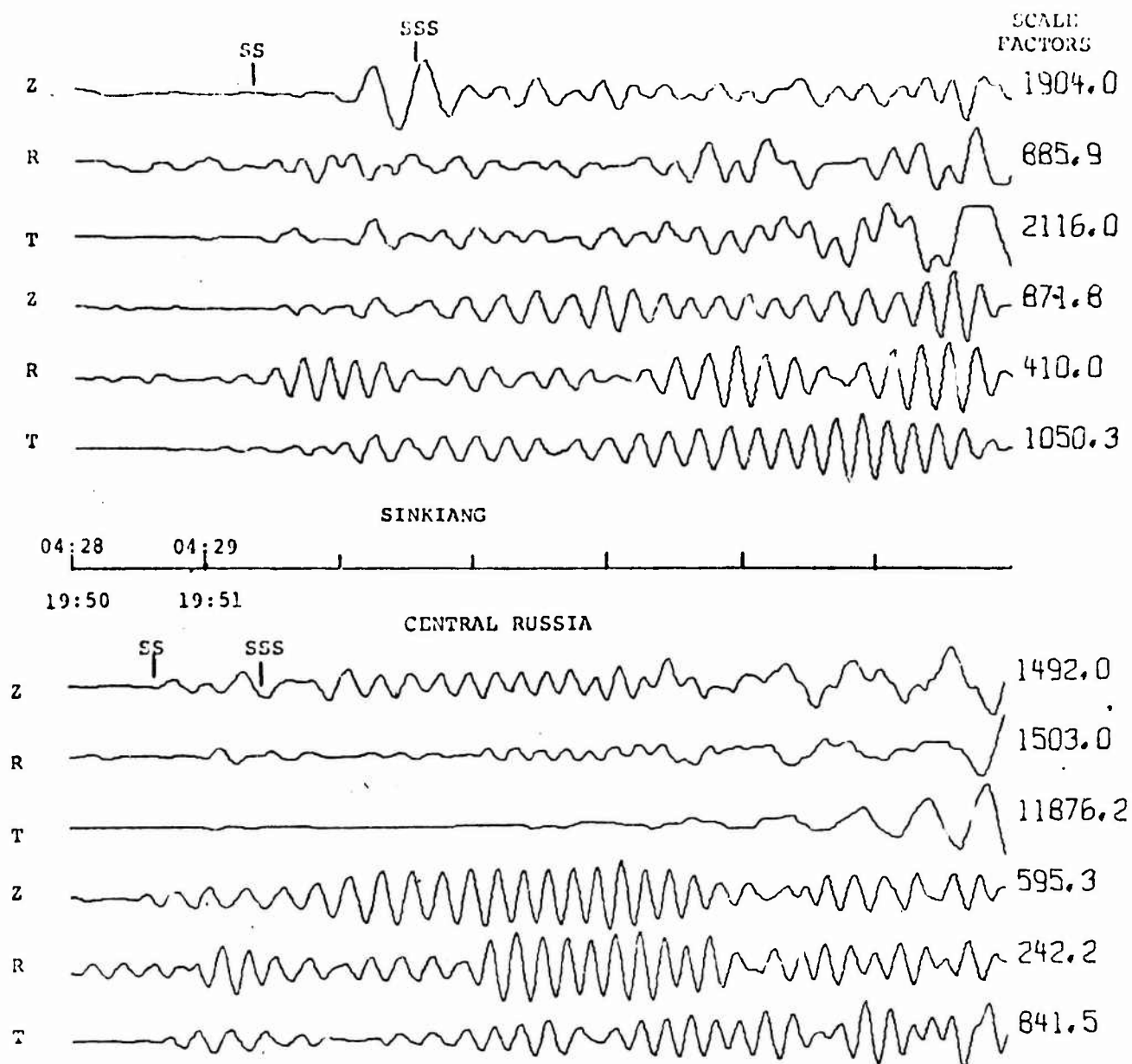
Fig. P.1

Higher mode wavetrains from events in Sinkiang (April 9, 1972, 04:10:50.7) and
Central Russia (August 24, 1971, 16:33:22.7). For each event, both unfiltered
and 8-17 sec bandpass filtered Z, R, T data from Subarray 01A is plotted.
Approx. JB times of body phases SS and SSS are marked.

Q.   SOURCE-SPECTRAL SCALiNG AND CORNER FREQUENCIES

Q.1 Earthquake Love-wave Spectral Ratios

The scaling of earthquake source spectra has been known
in an approximate way for some years, largely through the
work of Haskell (1964, 1966) and Aki (1967). In the present
work, the source factor of the far-field spectrum of Love
waves is being studied using the ω-square or ω-cube model
(Aki, 1967) as a starting point but not assuming the
principle of similarity to the same extent. The spectral
ratio method (Berckhemer, 1962) is applied wherein two or
more earthquakes with virtually the same focal location
are used and ratios of pairs of their Love-wave spectra
are determined, cancelling out instrument and path factors.

Aki's (1967) source spectral model was of one parameter,
presuming a one-to-one correspondence of M_s and m_b. In
this study a two-parameter model is assumed. This modified
model allows for M_s and m_b to vary independently. It is
expressed as

$$|A(\omega)| = \frac{k_o L^p}{[1+k_1\omega^2 L^2]^S [1+k_2\omega^2 L^2]^{\frac{1}{2}}} \qquad (Q.1)$$

where p and L are parameters and where $s = \frac{1}{2}$ or 1 according
as the ω-square or the ω-cube model is chosen as a starting
basis.

The expression for source spectral ratio then has four
independent parameters. The estimate of these four parameters
is then found from an algorithm which minimizes the variance
of the model spectral-ratio values with respect to the values
computed from the Fourier transforms of the two Love phases.
This has been done assuming a modified ω-square model as
well as a modified ω-cube model.

Although the theoretical spectral ratio is flat at high
and low frequencies, its steepness at intermediate frequencies
depends on the exponent of ι in the high-frequency asymptote.
When we apply the model of equation (Q.1) (actually the
ratio of two such expressions) to a group of deep-focus
Bonin Islands earthquakes, we get a better fit for s=1
(ω-cube) than for s=½ (ω-square). An example of this is
shown in Figures Q.1 and Q.2. In these figures the frequency
range, which extended to 0.5 Hz for the Fourier transform
output, is restricted to below 0.2 Hz because for higher
frequencies one of the spectra is predominantly noise.
The curves are extrapolated to 0.5 Hz but have no significance
beyond 0.2 Hz. They should in fact level off just above
the 1-level.

From Equation (Q.1), the corner frequencies of an event, ω_1
and ω_2, are defined as $(k_1 L^2)^{-\frac{1}{2}}$ and $(k_2 L^2)^{-\frac{1}{2}}$, respectively.
If these two corner frequencies (for one earthquake) differ,
then we have (assuming s=½) an intermediate ω^{-1} behaviour
as is present in models of Brune (1970) and Savage (1972),
among others. For the present data, however, ω_1 and ω_2 come
out virtually equal, implying that we have $k_1 \approx k_2$ in
equation (Q.1).

The corner frequencies determined so far agree in order of
magnitude with those of the ω-square and ω-cube models (Aki,
1967) at magnitudes around 5½ to 6, but there is some indica-
tion that p in equation (Q.1) may be greater than 3, its value
in Aki's models. This would imply a steeper corner-frequency
locus, that is, less variation of corner frequency with
earthquake size. This kind of behaviour has in fact been
incorporated into Aki's (1972) revised model Λ.

Q.2 Explosion Source Spectra and Discrimination

Clearly, the fundamental difference between earthquakes
and nuclear explosions is the difference in source mechanisms.
This ought to manifest itself in the source spectra and
indeed models of such for explosions (e.g., those of von
Seggern and Blandford, 1972) differ significantly from
those for earthquakes (e.g., those of Aki, 1967).

The Love-wave spectra from a group of Novaya Zemlya (pre-
sumed) explosions have been determined and an example of
their spectral ratio is shown in Fig. Q.3. It is fundamentally
different from the ratios of Figs. Q.1 and Q.2.
No attempt has been made to fit the modified ω-square
or ω-cube models to this data -- these models assume, as
a source, slip dislocation on a planar surface which is
obviously inapplicable to an explosion source.

R.J. Brown

REFERENCES

Aki, K. (1967): Scaling law of seismic spectrum, J. Geophys. Res.,
72, 1217-1231.

Aki, K. (1972): Scaling law of earthquake source time-function,
Geophys. J. R. Astr. Soc., 31, 3-25.

Berckhemer, H. (1962): Die Ausdehnung der Bruchfläche im Erdbebenherd
und ihr Einfluss auf das seismische Wellenspektrum, Gerl. Beitr.
z. Geophys., 71, 5-26.

Brune, J.N. (1970): Tectonic stress and the spectra of seismic shear
waves from earthquakes, J. Geophys. Res.,75, 4997-5009.

Haskell, N. (1964): Total energy and energy spectral density of elastic
wave radiation from propagating faults, Bull. Seism. Soc. Am.,
54, 1811-1842.

Haskell, N. (1966): Total energy and energy spectral density of elastic wave radiation from propagating faults, 2, A statistical source model, Bull. Seism. Soc. Am., 56, 125-140.

Savage, J.C. (1972): Relation of corner frequency to fault dimensions, J. Geophys. Res., 77, 3788-3795.

vcn Seggern, D., and R. Blandford (1972): Source time functions and spectra for underground nuclear explosions, Geophys. J.R. Astr. Soc., 31, 83-97.

LOVE-WAVE SPECTRAL RATIO BI60/58   FLETCHER-POWELL OMEGA-2
73 01 31   3-PT AVE LQ BI60 H=498 D=81.7 AZ=44.3   JB
73 01 15   3-PT AVE LQ BI58 H=477 D=83.0 AZ=44.1   JB
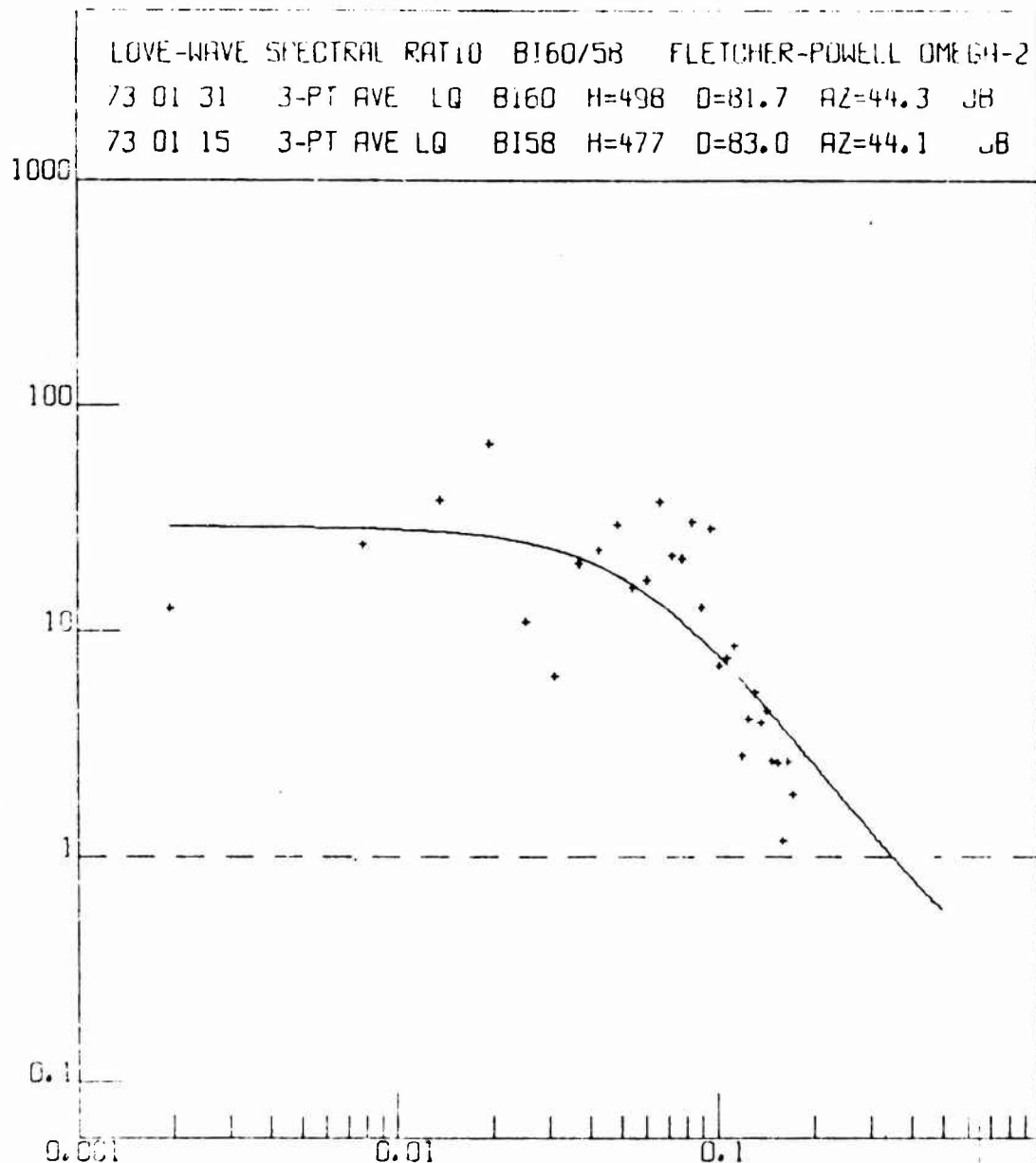
Fig. Q.1   Love-wave spectral ratio of two deep Bonin Islands
            earthquakes plotted versus frequency in Hz; computed
            by Fourier analysis of long period NORSAR Love-wave
            beam and group-averaged with three points to a group
            (plus signs); the curve is the least squares best fit
            assuming the modified ω-square model; S-wave corner
            frequency for the larger event (BI60) at 0.06 Hz.
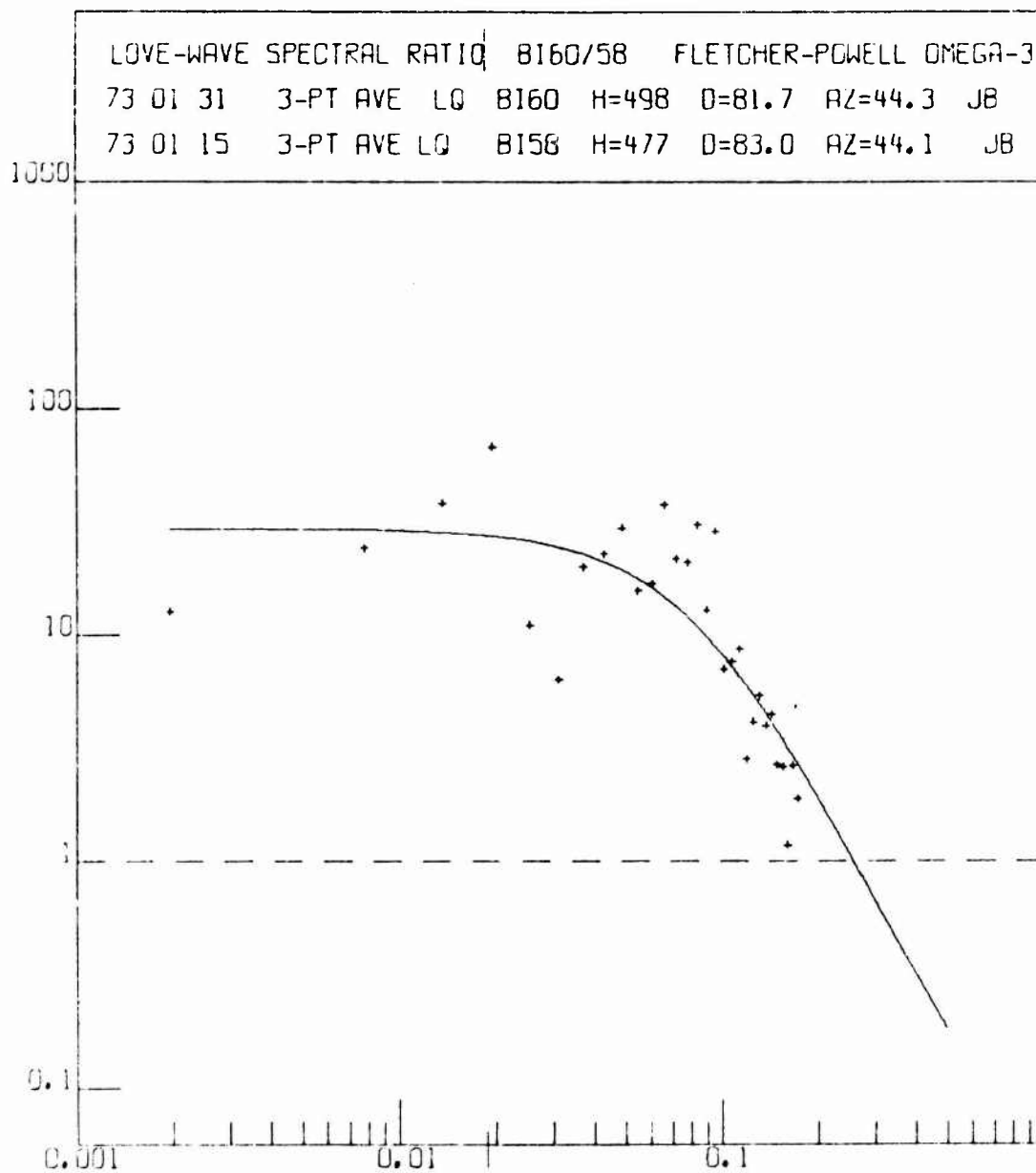
Fig. Q.2   Same as Fig. Q.1, but for the modified ω-cube model;
S-wave corner frequency of BI60 at 0.08 Hz.
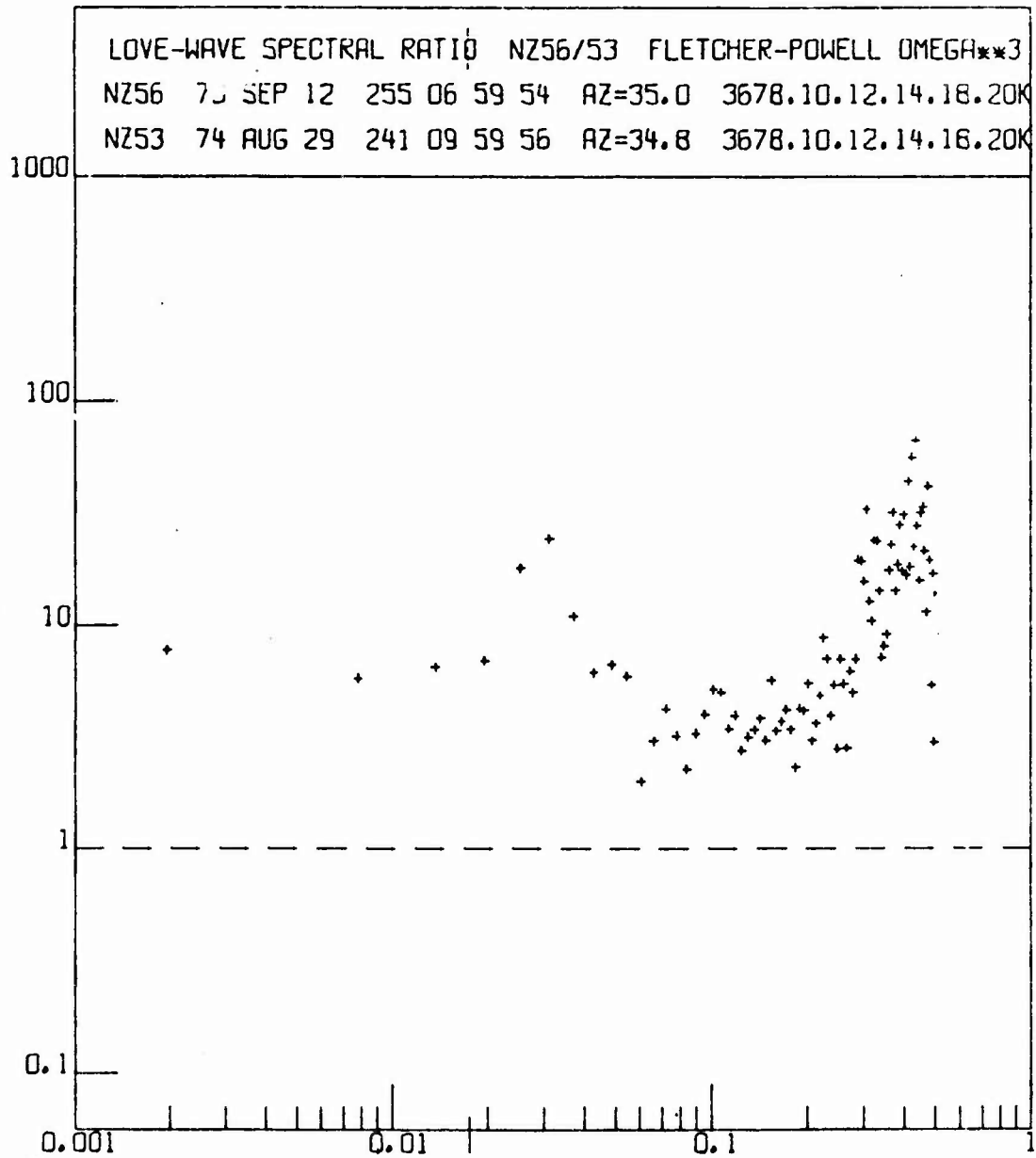
Fig. Q.3   Same as Figs. Q.1 and Q.2 for two Novaya Zemlya explosions;
            no model fit has been tried.

R.   IN SITU STRESS MONITORING

It has been known for some time now that several narrow
spectral peaks in the NORSAR short period recordings have
their origin in hydroelectric power plants in the vicinity
of the array. The exact nature of the generating mechanism
is not known, but it is characteristic that the seismic
spectral component is found at the very frequency of the
revolving mass, which is typically a few hundred tons. A
slight eccentricity in that mass could therefore account
for the leaked energy.

The most prominent contribution in this respect is obtained
near subarray 14C from the Hunderfossen power plant, which
has been found to generate a strong spectral component at
2.78 Hz, corresponding to 166 2/3 rpm. The location of this
steady-state energy source together with the closest seis-
mometers is shown in Fig. R.1, where it is seen that the
distances range from 4 to 14 km. In the initial analysis
of the data it was discovered that the frequency of the
desired spectral component was not stable; there were in
fact relatively rapid variations within the frequency range
2.774 to 2.781 Hz, so that an extensive Fourier analysis
was required just in order to locate the spectral peak. In
order to circumvent this problem, and to get a noise-free
source channel, a unit was built (at the University of
Copenhagen) which uses as input the 50 Hz, 220 v power, and
outputs a signal which is divided 18 times in frequency,
to 2.78 Hz, and scaled down to a voltage of ± 4.6 v. This
unit has now been hooked on to channel 14C05, thereby re-
placing the seismic data with a 2.78 Hz sine wave repre-
senting the source of the narrow spectral component.

The analysis of the data has so far only been preliminary,
involving spectral analysis of consecutive 3- minute intervals
over a time span of a few hours. It is noteworthy that the

introduction of the source channel reduced the required
computer time by almost a factor of 10, since a running
estimate of the frequency is now easily available; previously
it had to be estimated from the seismic data. Even with very
little blocking of data, we have obtained phase estimates
for the closest channels (1 and 2) with a stability of about
$\pm 1^0$, which corresponds to a precision of about $\pm 10^{-3}$ for
the distances involved in this experiment. In order to
monitor phase velocities, we have to study phase angle
differences, and Fig. R.1 shows that there are a number of
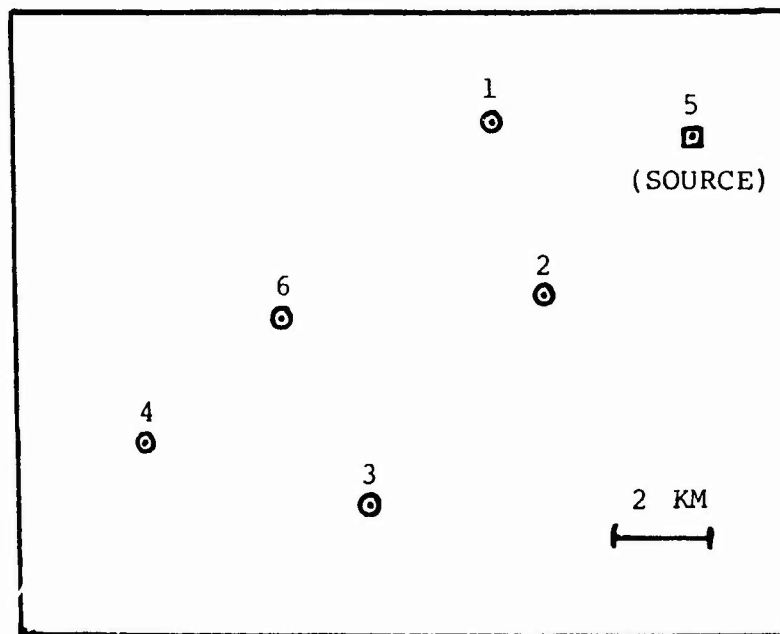
Fig. R.1   The relative locations of the Hunderfossen power plant
(source) and the 5 channels currently giving short period
seismic data from subarray 14C (circles). Seismometer
no. 5, which used to be located in the NW part of the
subarray, has been replaced by a sine wave representing
the source (see main text).

possible combinations. The most stable results have been
obtained using channels 1 and 2 in combination with the
source channel (5), even though there is an unknown phase
difference between the revolving mass and the generated
current, which we use as reference. For the other channels
(3 and 6) the loss in signal-to-noise ratio seems to be
about compensated for by the increased distance, yielding
the same relative stability.

By studying the distribution of the phase velocity dif-
ferences versus travel distance, it is not possible to
find any particular phase velocity which fits all the
data well. However, a velocity of about 5 km/s appears
to give the best overall fit. Because of the frequency
variation of the source we also get an independent
estimate of phase differences versus frequency, yield-
ing group velocity, and the few data obtained so far
have given estimates around 3 km/s both for combinations
1-5 and 2-5 (see Fig. R.1).

A computer program has now been developed which computes
the horizontal tidal strain in any particular direction
for the area around subarray 14C. We plan to continue this
experiment by looking for possible phase velocity dif-
ferences for different strain situations. The results
obtained so far indicate that by adding much larger amounts
of data, it could be possible to obtain phase difference
estimates with a precision closer to 10^{-4}.

H. Bungum,

K. Aki (Cambridge, U.S.A.)

T. Risbo (Copenhagen, Denmark)

S. EARTHQUAKE ACTIVITY IN FENNOSCANDIA, 1497-1973

The systematic collection of macroseismic data on earthquake occurrence in Fennoscandia began in the 1880's when the use of questionnaires was initiated. Prior to that time macroseismic information is fragmentary and incomplete although the essential data on the larger earthquakes during another 300-400 years have been preserved. Using all pertinent macroseismic and seismograph data available, we have constructed new seismicity maps for Fennoscandia covering the time interval 1497-1973. Since the quality of macroseismic as well as instrumental data is a function of magnitude, we have constructed these maps for different magnitude intervals. Fig. S.1 shows the epicenter distribution for earthquakes with magnitude above 4.5, and the activity has been subdivided in four broadly defined zones; the Telemark-Vänern, the Western Norway, the Bothnian and the Lappland zones. There is no clear correlation between available geological and geophysical information and the earthquake occurrence, and this also applies to the Oslo Graben region. The on-going tectonic processes causing the earthquakes are not at all well-understood, and particularly so since fault plane solutions have not been obtained for any Fennoscandian earthquake.

E.S. Husebye, H. Gjøystdal,
H. Bungum
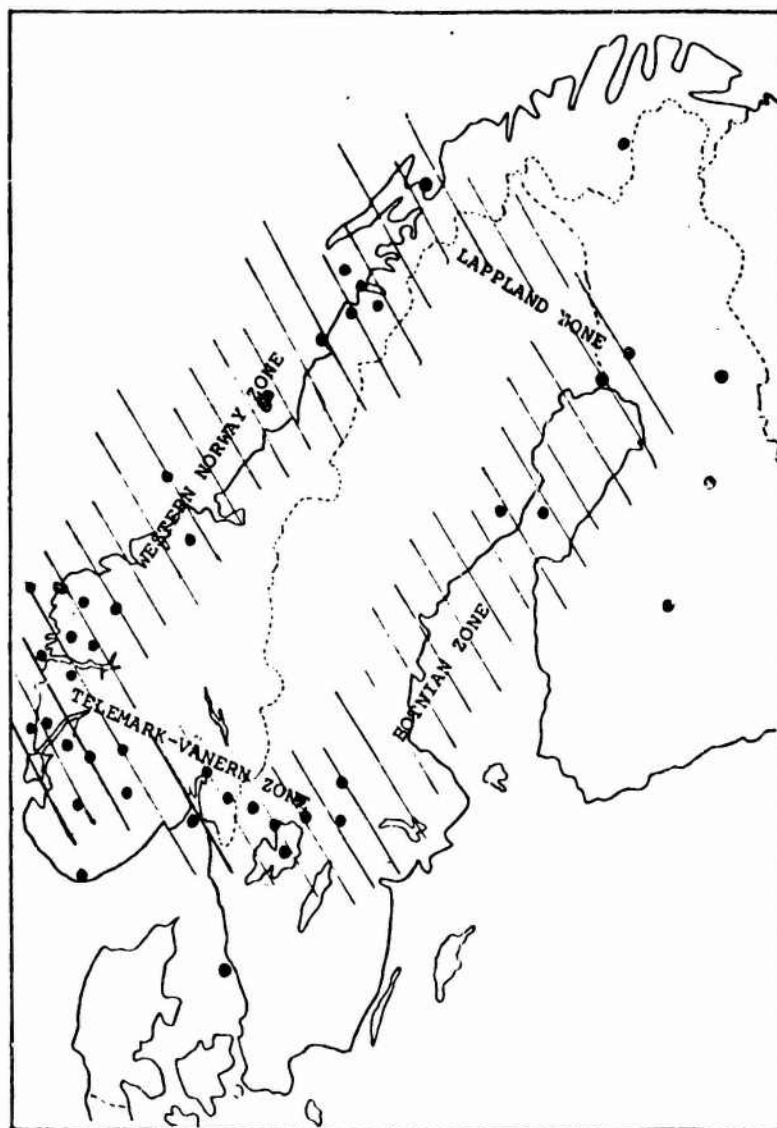
Fig. S.1 Epicenter map of Fennoscandian earthquakes (magnitude $\geq$ 4.5) for the period 1497-1973. Hatched areas indicate the proposed major seismicity zones.

T.   DETECTION PROCESSOR OPERATION

The Detection Processor system has been run and operated
with the goal of having minimal system down time within
the reporting period. The up time percentage is thus 99.2%
for this period, as compared to 97% for the last reporting
period (January - June 1974). The causes of breaks in
the recording have mainly been hardware problems. A float-
ing threshold procedure has been introduced, computing
periodically a noise stability estimate. The low priority
message task has been split into overlays, to obtain
space for future additions to DP.

T.1 Data Recording and DP Down Time

Fig. T.1 and the accompanying Table T.1 show the daily
DP down time in hours for the days between 1 July 1974 and
30 June 1975. The monthly recording times and percentages
up are given in Table T.2. The most significant break,
as seen from Fig. T.1, occurred on June 26, when a power
failure had introduced an error in the SPS hardware. The
DP went down 3 times, giving a total down time of 3 hours
on the 25th and a little more than 11 hours on the 26th.
On March 10 a case of "SPS interrupts not received by the
DP" caused the system to be down more than 6 hours. On
August 9, 1974, the SPS went down, indicating high tempera-
ture (THERM - FR 1 on), giving a break of 5½ hours.

Additionally, we have a relatively even spread of down
time throughout the period. However, if we look at the
column giving "DAYS WITH BREAKS", we will see that this
number has been low after January this year. Since repeated
breaks within a day very often have the same cause, the
decrease of this number indicates better conditions towards
the end of the period. The 130 breaks listed in Table T.1
can be separated into the following groups, according to
the cause of the break:

SPS problems	:	23
Software problems	:	22
TOD problems	:	21
Other hardware (CPU, 2701, etc.)	:	15
Power breaks & jumps	:	12
Tape drive problems	:	10
Disk drive problems	:	7
CE work	:	7
Program change	:	6
Tests	:	3
ARPANET TIP	:	2
Unknown	:	2

The "Software problems" category consists mainly of situations when, for some reason not yet understood, the system timing printed out on the 1052 console typewriter is completely wrong. To correct this, the system has to be taken down and up again. A malfunctioning Time-of-Day (TOD) unit was the cause of many recording irregularities and breaks, until the error was tracked down and fixed in the beginning of February this year. It has worked correctly since that time. Apart from these two categories, the predominant causes of DP going down have been hardware problems. The case of the SPS not sending an interrupt when it should is the major single cause of DP going down. The total down time for this period was 74 hours 15 minutes. The over-all mean time between failures, which is the sum of the uptime intervals, divided by the number of breaks plus one, was 2.8 days, as compared with 1.7 days for the last reporting period (January - June 1974).

T.2   DP Algorithms and Parameters

Two changes have been performed in the programs making up the Detection Processor. The Low Priority Message task has been implemented as a set of overlays, in order to make room

for the future implementation of the Network Control Program
task. A floating threshold procedure has been coded into
the detection task. An estimate of the noise stability is
computed periodically, to be ultimately passed to the Event
Processor in a signal arrival record.

D. Rieber-Mohn
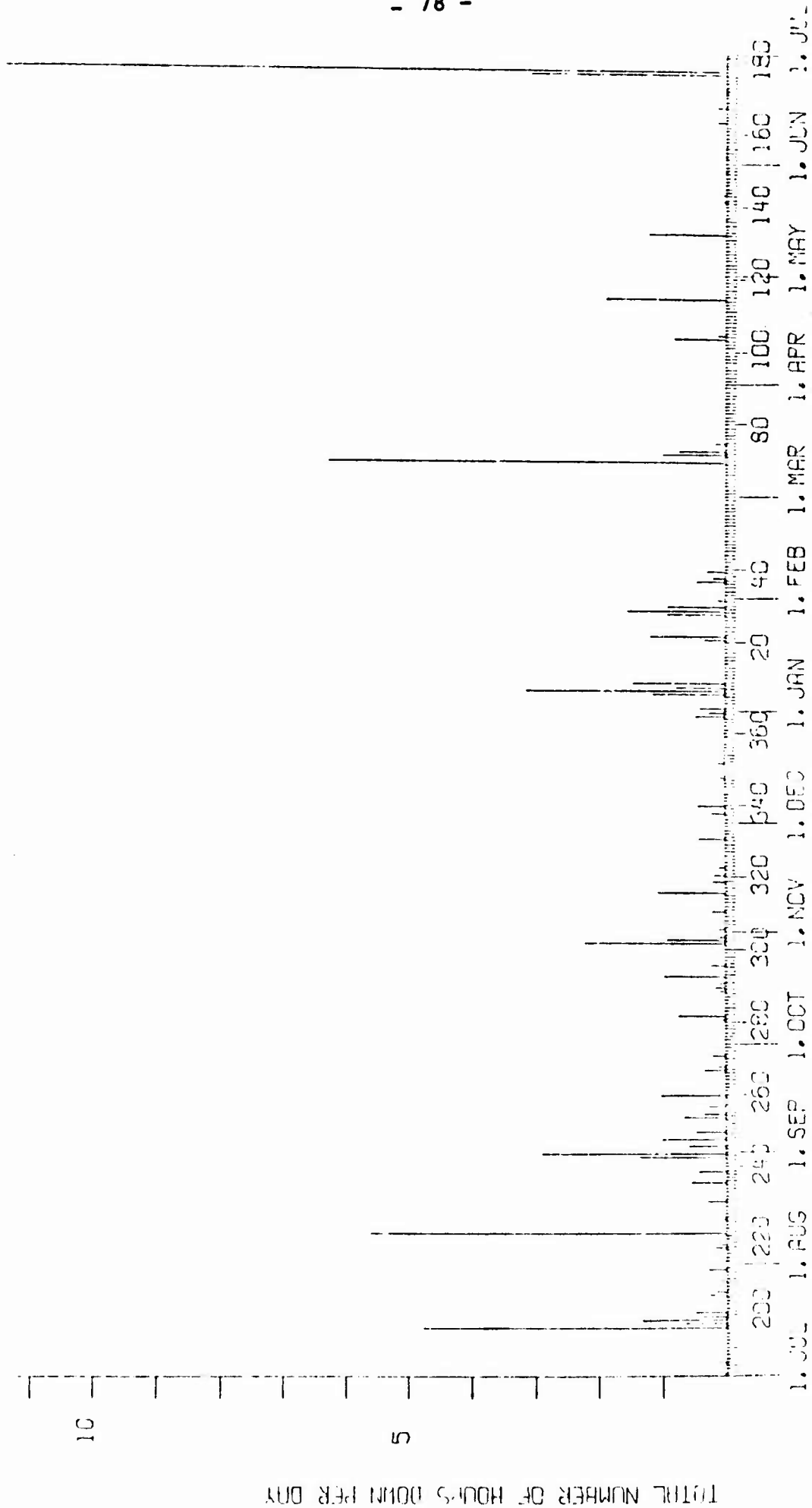
Fig. T.1 Detection Processor down time in the period 1 July 1974 - 30 June 1975.

TABLE T.1

List of breaks in DP processing in the period 1 July 1974 - 30 June 1975.

LIST OF BREAKS IN DP PROCESSING THE LAST YEAR

DAY	START		STOP		COMMENTS..........
102	9	55	9	57	CHANGE OF TAPE UNITS
185	12	3	12	11	CHANGED TOD UNIT
195	11	29	14	35	POWER BREAK
195	20	55	22	14	CPU FAILURE A TO B
196	9	24	9	38	POWER FAILURE ON B
196	15	12	15	37	SPS INTER NOT RECEIVED
197	1	55	2	37	POWER ON A CAUSE B STOP
197	20	57	21	15	2701 FAILURE
198	22	25	22	48	2701 POWER TROUBLE
199	7	4	7	11	2701 FAILURE
199	13	33	13	47	270. FAILURE, SPS I.N.R.
199	17	10	17	27	TOD FAILURE
204	14	30	14	46	POWER JUMP
205	3	33	3	43	1052 TIMING WRONG
208	8	19	8	24	1052 TIMING WRONG
211	15	25	15	42	1052 TIMING WRONG
217	0	42	0	52	SPS INTER NOT RECEIVED
218	12	25	12	30	PROGRAM CHANGE
221	0	17	0	55	SPS HIGH TEMPERATURE
221	1	17	6	15	SPS HIGH TEMPERATURE
225	8	35	8	41	1052 TIMING WRONG
230	1	28	1	46	TOD ADJUSTMENT
235	3	25	3	33	2701B POWER FAILURE
235	11	53	12	13	PROGRAM TEST
238	9	56	10	12	TAPE INDICATE ON 153
238	10	27	10	37	POWER FAILURE
242	21	57	23	19	POWER OFF FOR B
243	18	10	21	11	CHANNEL 1 HANGING
245	8	2	8	13	BAD TAPE UNIT 252
245	9	5	9	29	TEST ON TAPE UNIT 272
247	10	51	11	5	SPS INTER NOT RECEIVED
247	12	9	12	30	PROGRAM ERROR
247	12	47	12	50	PROGRAM ERROR
247	13	58	14	12	PROGRAM ERROR
249	13	4	13	32	PROGRAM ERROR
253	8	0	8	28	PROGRAM ERROR
253	14	16	14	35	PROGRAM ERROR
254	13	14	13	35	PROGRAM ERROR
256	10	20	10	43	PROGRAM ERROR
259	20	26	21	27	POWER BREAK
266	8	0	8	20	CHANGE OF TAPE DRIVES
267	9	9	9	15	PROGRAM CHANGE
270	11	44	11	56	PARAMETER CHANGE
280	9	15	9	16	CHANGE OF TAPE DRIVES
281	16	15	16	59	1052 TIMING WRONG
288	8	55	9	1	1052 TIMING WRONG
289	9	57	10	9	CHANGE OF TAPE DRIVES
290	7	26	7	31	1052 TIMING WRONG
292	12	56	13	56	T.U. 272 CAUSED HANGUP
295	17	5	18	5	PUNCH UNIT CHECK
301	8	56	9	10	T.U. 252 CAUSED HANGUP
301	18	55	20	25	DISK DRIVE 242 TROUBLE
301	22	55	23	19	DISK DRIVE 243 TROUBLE
302	6	5	7	6	DISK DRIVE 242 TROUBLE
302	8	31	9	11	DISK DRIVE 242 TROUBLE
303	9	25	9	50	CHANGE OF DISK PACK
305	12	2	12	6	CHANGE OF DISK DRIVES
310	7	52	8	5	CE WORK
315	3	48	4	52	POWER FAILURE
316	12	52	13	5	CE WORK

Sheet 1 of 3

LIST OF BREAKS IN OP PROCESSING THE LAST YEAR

DAY	START		STOP		COMMENTS...........
320	0	1	0	12	DISK DRIVE TROUBLE
322	17	30	17	36	TOD ADJUSTMENT
330	14	22	14	47	CE CAUSING MACHINE CHK
337	8	54	9	2	PROGRAM CHANGE
337	10	45	10	49	PROGRAM CHANGE CORR.
339	10	13	10	15	CHANGE OF TAPE DRIVES
339	20	55	22	0	CHANNEL HANGUP
347	6	42	6	48	1052 TIMING WRONG
351	6	56	7	2	PROGRAM CHANGE
364	9	45	10	13	CE WORK
365	23	45	24	0	TOD ADJUSTMENT
1	0	0	0	10	TOD ADJUSTMENT
1	1	14	1	20	1052 TIMING WRONG
1	3	2	3	10	1052 TIMING WRONG
5	3	24	4	32	CPU ERROR A TO B
6	6	0	6	10	UNKNOWN
6	10	46	10	54	TOD FAILURE B TO A
6	11	29	11	45	TOD FAILURE
6	13	55	14	14	CPU ERROR A TO B
6	16	23	18	12	CE WORK
6	18	35	19	0	CE WORK
7	11	45	11	55	TOD ADJUSTMENT
7	17	35	18	8	TOD ADJUSTMENT
7	18	13	18	16	SPS INTER NOT RECEIVED
8	7	19	7	35	TOD ADJUSTMENT
8	10	56	11	3	TOD ADJUSTMENT
8	11	24	11	37	TOD UNIT CHANGED
8	14	9	14	40	TOD ADJUSTMENT, B TO A
20	9	28	9	33	TIP POWER OFF
20	12	3	12	47	ARPANET INTERFACE TEST
21	9	45	10	35	POWER FAILURE A TO B
21	13	40	13	52	INTERFACE TEST B TO A
21	14	39	14	49	TIP POWER OFF
27	12	32	12	49	TOD INCORRECT
27	14	47	14	56	TOD INCORRECT
27	15	21	15	43	TOD INCORRECT
28	21	35	23	7	POWER JUMP
29	8	28	8	56	TOD INCORRECT
29	13	6	13	24	TOD INCORRECT
31	13	2	13	10	TOD ADJUSTMENT
36	10	56	11	25	POWER JUMP
37	9	7	9	10	TOD ADJUSTMENT
37	12	56	13	5	SPS C3 FRAME 2 POWER
39	12	9	12	26	CE WORK
69	3	55	10	12	SPS INTER NOT RECEIVED
71	14	37	14	47	SPS INTER NOT RECEIVED
71	19	32	19	37	SPS INTER NOT RECEIVED
71	20	15	20	47	SPS INTER NOT RECEIVED
71	23	47	24	0	SPS INTER NOT RECEIVED
72	0	0	0	9	SPS INTER NOT RECEIVED
72	1	0	1	22	SPS INTER NOT RECEIVED
72	2	33	2	44	SPS INTER NOT RECEIVED
72	3	48	4	2	SPS INTER NOT RECEIVED
74	10	20	10	30	UNKNOWN

Table T.1
Sheet 2 of 3

LIST UF BREAKS IN UP PROCESSING THE LAST YEAR

DAY	START		STOP		COMMENTS...........
103	8	17	8	28	SPS INTER NOT RECEIVED
103	8	49	9	26	SPS INTER NOT RECEIVED
104	1	33	1	40	SPS ERROR,WRONG TODTIME
114	13	47	3	56	SPS INTER NOT RECEIVED
114	14	10	14	32	SPS INTER NOT RECEIVED
114	14	34	14	56	SPS INTER NOT RECEIVED
114	15	11	15	34	SPS INTER NOT RECEIVED
114	15	4.	.0	0	SPS INTER NOT RECEIVED
114	20	29	20	47	SPS INTER NOT RECEIVED
132	4	20	5	38	1052 ERROR A TO B
141	11	32	11	35	B TO A
143	10	17	10	29	POWER JUMP
163	8	0	8	8	LINEPRINTER 640,A TO B
167	7	50	7	58	B TO A
176	20	58	24	0	SPS ERROR,POWER FAILURE
177	0	0	1	3	SPS ERROR,POWER FAILURE
177	1	30	2	50	SPS ERROR,POWER FAILURE
177	4	58	13	56	SPS ERROR,POWER FAILURE

Table T.1
Sheet 3 of 3

TABLE T.2

DP and EP Computer Usage 1 July 1974 - 30 June 1975.

Month	DP Uptime (hrs)	DP Uptime (%)	No. of DP Breaks	No. of Days with DP Breaks	DP MTBF	EP Uptime (hrs)	EP Uptime (%)
Jul 74	738	99.1	16	11	1.9	336	45.3
Aug 74	733	98.5	12	9	2.6	264	35.5
Sep 74	715	99.3	15	10	2.0	200	27.8
Oct 74	739	99.3	13	10	2.4	225	30.2
Nov 74	718	99.7	7	7	4.3	218	30.3
Dec 74	742	99.8	88	6	3.9	191	25.7
Jan 75	732	98.4	29	11	1.1	175	23.5
Feb 75	671	99.9	4	3	7.0	198	29.5
Mar 75	736	98.9	9	4	3.4	166	22.3
Apr 75	717	99.6	9	3	3.3	233	32.4
May 75	743	99.8	3	3	10.3	167	22.4
Jun 75	705	98.0	5	4	5.9	236	32.8
Total	8688	99.2	130	81	2.8	2609	29.8

U.   EVENT PROCESSOR OPERATION

U.1   General Considerations

The operation of the Event Processor system (EP) has in this
period been somewhat hampered by malfunctioning hardware
(Tape drives, 2260 console, disk drives) and improper input
data from disk files and tapes. Since the EP is strongly
tape-dependent, the recurring problem of tape read data
check causes a deterioration in the performance.

U.2   Computer Utilization

During the period July-December 1974 the EP was up 32.5%
of the time, and for January-July 1975 the percentage was
27.2, which is the lowest ever recorded. Two changes in
the EP programs in this last year have influenced the pro-
cessing time: Firstly, a new package has been developed
which is executed for some of the events in order to perform
some statistical tests and a possible weighted beamforming.
This should increase the computer time per event, while
the statistics show that the time per processed detection
and especially the time per accepted event has never been
smaller. This can be explained by the second change, namely,
the floating EP acceptance threshold. Although the number
of processed detections is still about the same, the number
of false alarms has decreased and the relative number of
accepted events has increased. Since the false alarms (noise
detections) always require more computer time, this can
explain the increased efficiency of the EP.

U.3   EP Operational Problems

No special operational problems have occurred in this period,
apart from the infrequently occurring breakdowns because
of bad input data from the shared disk files or tapes. Bad
detection times are especially malicious, because the effects
of reading such times propagates through the system. Another
source of operational problems is malfunctioning hardware,
such as tape drives, disk drives and the 2260 console station.

U.4 EP Parameters and Algorithms

The following changes have been made to the Event Processor system within this period:

A new program package was added on December 2. This package (SP8) will be invoked by weak events with signal-to-noise ratios just above the pre-processing threshold. Three different test statistics will be computed, to aid the analyst in his signal-noise decision. Depending on the value of the first statstic a weighted array beamforming will be performed, using optimum subarray beam weights.

The results of the three tests and the optimum weights will be printed in the Summary Report for the event. Also, the weighted array beam is plotted on the event's plot panel.

On December 16 changes were introduced in the EP controller, in order to compute periodically a "floating" signal-to-noise ratio pre-threshold for the coherent detections. A noise stability estimate (STAB) is received with each signal arrival, as read from the Signal Arrival File on the Shared Disk pack. Together with the desired false alarm rate (FAR) inserted by the operator at start-up time, the pre-threshold value (TH) is computed as follows:

$$TH = 12.08 - 0.89 \log (FAR) - 0.18 \, STAB$$

This computation is performed each time a new value of STAB differs from the earlier one, which means that the noise stability, as computed by DP, has changed. The actual computation of TH is done in a separate FORTRAN overlay phase, loaded and invoked by the EP controller each time it is used.

On January 4 an option to invoke the SP8 package for a re-
run was introduced in MJRRUN, the re-run initialization
program.

On March 4 a small subroutine (SPCONV) was added to the
Detection Bulletin Report package. Instead of doing a
dummy read statement (from data set zero) in SPRELSE, using
PFIOCS and IOCS for a format conversion, the new subroutine
performs just this. The earlier technique did not seem to
work on all occasions and caused EP to terminate at this
point.

On May 15 the Partial Array Beam list in EP Common was
changed upon request from Vela Seismological Center.
The Partial Array Beams (PABs) were changed to be as
follows:

PAB 1 = Subarray Beam 01A
PAB 2 =   "   "   03C
PAB 3 =   "   "   07C
PAB 4 =   "   "   13C

At the same time the lower limit for the computed "floating"
pre-threshold of coherent detections was lowered from
3.4 to 3.2.

U.5   EP Performance Statistics

Summaries of analyst decisions for each of the two half
years in this reporting period are given in Tables U.1 and
U.2. The only significant change from previous reporting
periods is the drop in the number of false alarms after the
floating threshold procedure was implemented late in
December 1974. The main effect there, however, is not so
much on the total number of false alarms but on the
distribution: there is now about equally many false alarms
every day regardless of noise conditions. This avoids the

processing of a large number of noise detections during microseismic storms, and normally it should also pick up some additional events during quiet periods. As mentioned above, it has resulted in a more efficient utilization of the computers: the EP up time per accepted event is now at an all time low.

The number of reported events on a monthly basis is given in Table U.3, and the distribution on a daily basis is shown in Fig. U.1. The large number of events in August 1974 is due to an earthquake swarm from the Tadshik-Sinkiang region, while swarms from Japan and the Kuriles can explain the large number of events in June 1975.
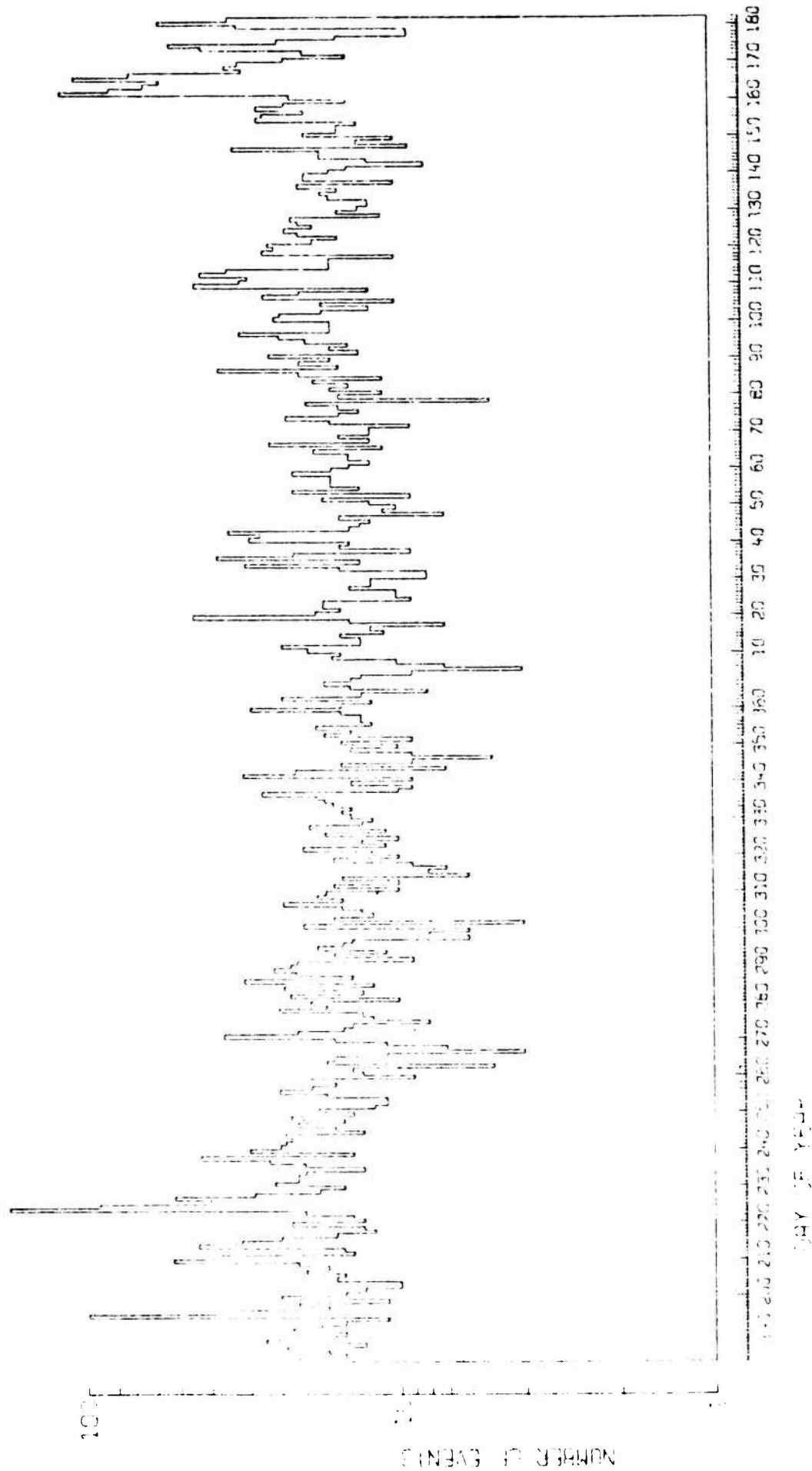
Fig. U.1   Number of events as a function of day of year July 1974-June 1975.

TABLE U.1

Analyst decisions for detections processed by EP during the
time period July-December 1974.

Analyst Classifications	Number of Processings	Percentage
Accepted as events	3798	48.4
Rejected as being		
- Poor SNR or noise	1910	24.3
- Local events	905	11.5
- Double processings	796	10.2
- Communication errors	436	5.6
Sum Processed	7845	100.0

TABLE U.2

Analyst decisions for detections processed by EP during the
time period January-June 1975

Analyst Classifications	Number of Processings	Percentage
Accepted as events	3929	53.2
Rejected as being		
- Poor SNR or noise	1039	14.1
- Local events	1213	16.4
- Double processing	723	9.8
- Communication errors	476	6.5
Sum Processed	7380	100.0

TABLE U.3

Number of teleseismic and core phase events reported during the time period July 1974-June 1975.

Month	Teleseismic	Core	Sum
Jul 74	532	151	683
Aug	851	106	957
Sep	374	83	457
Oct	394	81	475
Nov	318	91	409
Dec	369	79	448
Jan 75	346	80	426
Feb	391	92	483
Mar	401	89	490
Apr	525	111	636
May	402	93	495
Jun	1003	80	1083

V. PROGRAMMING ACTIVITY

The programming group consisted of 5 persons at the outset
of this period, but was reduced to 4 at the start of 1975.
A further reduction of one person occurred at the end of
this period. The group has been involved in the following
activiti?s:

-   new programming developments
-   maintenance and improvement of existing programs
    and program systems
-   routine processing of utility and application piograms
-   consultation support
-   use of the ARPA network and related studies.

The maintenance of the program systems and the use and study
of the ARPA network is described elsewhere in this report.

V.1 Development of New Programs

The following programs have been designed and coded in this
period:

-   a program that, based on a card-punched input of the
    DP down time history of a certain period, computes
    various parameters and plots a diagram giving down
    time each day (N/PD-69, DPDWN),
-   a FORTRAN compatible tape write routine for writing
    binary records of arbitrary length on a tape (N/PD-70
    WRTREC),
-   A FORTRAN compatible routine for forward or backward
    spacing of files on a multifile tape (N/PD-71, POSTAP),
-   a program for computing channel responses for given
    frequencies, based on a model parameter set or a set
    given by the user (N/PD-72, DCRESP),

- a set of programs designed to extract NR-records
  from NORSAR Low Rate tapes and copy them onto NORSAR
  Data Retention Low Rate tapes (N/PD-73, LRINPUT/
  LRSTACK/LRLSTPCH),
- a set of FORTRAN disk pack I/O routines that makes
  it convenient to store and retrieve real data, using
  a disk pack (N/PD-74, SKRIV/LES),
- a program that plots 3 - component long period NORSAR
  data for up to 22 subarrays, and optionally performs
  azimuthal rotation and zero phase filtering (N/PD-75,
  LPSUBS),
- a program that plots the data on the recording tapes
  from the Kongsberg High-gain, Broadband, Long Period
  Seismograph Station (N/PD-76, KBPLOT),
- a program for plotting time series from High or Low
  Rate tapes, from various sources (NORSAR, LASA, or
  ALPA), filtered or unfiltered (N/PD-77, TSPLOT),
- a subroutine for converting data from gain ranged
  to integer format (N/PD-78, FIXIT),
- a program for code conversion of punched card source
  decks (N/PD-79, CONVRT),
- a subroutine that reads NORSAR Long Period data from
  NORSAR Low Rate tapes (N/PD-80, LOWRAT),
- a subroutine that reads LASA or ALPA Long Period data
  from NORSAR Low Rate tapes (N/PD-81, LASA).
- In addition other programs for various applications have
  been developed. Programs received from other institu-
  tions have been adapted for use at NORSAR, as for
  instance a program received from SDAC for checking
  out a Special Host Interface Unit, a program for
  three-dimensional plotting (Algorithm 420 in CACM
  vol 15, no. 2, Feb 1972), and the international
  Mathematical and Statistical Library's Utility Program,
  UBLIBM.

V.2 Routine Processing

Various forms of routine processing have been undertaken
by members of the Programming group, to monitor the follow-
ing activities:

- maintenance of the NORSAR Tape Library directory
- discrimination tests and explosion data compilation
- data retention for High Rate, Low Rate and Detection
  Log data. This involves selecting data to be saved
  permanently, and stacking them on so-called data
  retention tapes, at the end of the original retention
  period.
- supervision and execution of sporadic run requests
  for different programs, from scientists, visitors
  and other institutions.

D. Rieber-Mohn

W.   THE NORSAR ARPANET CONNECTION

The Terminal Interface Processor (TIP) located in the NORSAR
Data Processing Center is a node in the ARPA Network. Two
terminals (Tektronix 4010-1 and Data Dynamics 390) have
been attached to the TIP during this period.

The NORSAR bulletin has routinely been converted to paper
tape and inputted through the Data Dynamics 390 terminal,
to be transmitted to the message file of the U.S. Geological
Survey on the OFFICE-1 Host computer at Stanford, California,
thus speeding up delivery and keeping the bulletin in a
format which is directly machine-readable.

The terminal access has also been used for information
exchange with other institutions (Seismic Data Analysis
Center, Lincoln Laboratory's Seismic Discrimination Group,
U.S. Geological Survey, Vela Seismological Center, etc.).
This activity is based on our account on the SRI-ARC
(Stanford Research Institute's Augmentation Research
Center) computer, and the use of this system's facilities
and resources. In the middle of this period our account was
transferred to the OFFICE-1 computer, at the closing down
of the SRI-ARC computer.

In the beginning of January, two Special Host Interface
Units for the 360 machines were installed, thus physically
linking the multiplexor channel of each IBM/360 machine to
a corresponding General Host Interface within the TIP. A
program called "WRABBIT" was received over the ARPANET
from SDAC and was, with small modifications, used to check
out the Host-TIP connections through the installed units.

During the last six months of the reporting period, a
first version of a Network Control Program, dedicated to
data exchange with the forthcoming Communications and Control
Processor (CCP) has been developed to be implemented as a
task in the Detection Processor System. This task <u>has</u> been
implemented and tested out in the so-called Secondary
On-line System (SOS), which actually is a copy of the
Detection Processor System, used for experimental purposes.
The SOS now sends error-free messages to itself over the
ARPANET. Also, test sessions have been started, where we
have run the SOS, to let it exchange messages with the
program in the CCP, presently situated at BBN in Boston,
Mass. Some minor discrepancies in the interpretation of
protocol were discovered and cleared up. Also, a time
discrepancy was discovered.

We are now ready to start up these test sessions again, and
expect to test the NCP-task in a more realistic environment,
with full processing load on DP at the same time as we
exchange messages over the network. A plan for implementation
of a Network Control Program of the off-line (B) computer
has been worked out, in which we expect to use 7 man-months
to perform this job. With the anticipated staff reduction
for the next period, this work load estimate may turn out
to be too small.

D. Rieber-Mohn

X.   NORSAR DATA PROCESSING CENTER (NDPC) OPERATION

X.1 Data Center

No substantial change in equipment configuration occurred
in the period, except for the installation of two ARPANET/
IBM 360 interface units (see Section W).

Operation and maintenance continued in accordance with
established routines and schedules. Two new operators
were hired as replacements for personnel leaving the pro-
ject.

In spite of a more intensive care of the equipment, rather
frequent failures and malfunctions occurred, in particular
of peripherals. Also, a tendency towards more frequent
stops of the Special Processing System (SPS) has been
observed.

The Time-of-Day (TOD) generator has caused some concern,
mainly due to periodic absence of the accurate comparison
signal from the nearby Air Force base, caused by faulty
equipment. Further experiments have been made with the WWV
receiver and various antennas, however, usable signals
cannot be obtained due to bad local reception conditions.

X.2 Communications

A summary of communication outages is given in Table X.1.
The high outage of 01C is caused by a power outage (broken
ground cable) rather than communication failure. Otherwise,
the average outage is about "normal". Lines with degraded
performance are defined as those having between 20 and 200
errors in a 16-minute interval as seen on the printout.
More than 200 errors in the same interval causes masking
and outage of the subarray.

TABLE X.1

Communications, degraded performance/outages. Monthly figures in hours. Month= 4 or 5 week period as indicated.

Sub-area	JUL(4)		AUG(5)		SEP(4)		OCT(5)		NOV(4)		DEC(4)		Total 4 year		Per cent 4 year	
	>20	>200	>20	>200	>20	>200	>20	>200	>20	>200	>20	>200	>20	>200	>20	>200
01A	2.5	0.7	1.0	0.8	0.3	0.7	1.7	2.7	2.0	--	0.7	--	8.2	4.9	0.2	0.1
01B	1.8	2.5	2.0	0.8	1.0	0.3	3.7	3.0	1.8	--	1.5	--	11.8	6.6	0.3	0.2
02B	2.0	0.7	1.3	0.8	1.0	0.3	1.0	2.5	1.5	--	1.3	31.6	8.1	35.9	0.2	0.8
03B	2.2	0.7	1.7	0.8	0.3	0.3	1.3	2.5	1.2	--	1.0	1.7	7.7	6.0	0.2	0.1
04B	1.8	1.7	1.0	0.8	0.7	0.3	1.8	11.4	1.5	--	1.3	--	8.1	14.2	0.2	0.3
05B	14.8	2.9	12.8	13.8	18.5	9.9	30.7	7.2	59.3	0.7	24.2	0.8	160.3	35.3	3.7	0.8
06B	5.7	3.9	4.0	4.0	1.5	8.2	1.8	6.6	2.7	1.5	2.7	4.7	18.4	28.9	0.4	0.7
07B	7.2	20.3	3.9	78.3	3.0	7.2	2.2	6.9	2.5	1.5	2.5	1.5	21.3	115.7	0.5	2.6
01C	2.7	115.0	2.7	4.4	1.8	13.8	2.2	9.2	1.5	43.3	1.7	1.3	12.6	187.0	0.3	4.3
02C	14.3	2.4	12.1	7.7	6.2	2.9	16.6	3.0	9.2	2.5	8.1	1.3	66.5	19.8	1.5	0.5
03C	8.2	87.7	1.0	0.8	0.7	1.5	1.3	2.9	1.5	0.5	2.9	1.2	15.6	94.6	0.4	2.2
04C	2.2	106.2	2.7	0.8	--	0.3	0.7	3.2	0.8	16.5	0.7	--	7.1	129.0	0.2	3.0
05C	1.5	396.1	1.2	2.2	0.3	1.0	1.0	2.5	1.8	0.7	1.8	2.7	7.6	405.2	0.2	9.3
06C	0.7	0.3	1.0	45.9	0.7	1.3	0.7	16.4	1.5	40.5	1.0	2.7	5.6	107.1	0.1	2.5
07C	37.0	3.5	60.6	3.7	18.3	1.0	0.3	1.5	1.7	4.0	0.3	--	118.2	13.7	2.7	0.3
08C	--	--	1.8	1.2	2.5	7.1	4.5	16.3	8.7	15.6	4.4	8.7	21.9	48.9	0.5	1.1
09C	4.9	22.0	2.5	3.7	1.8	6.9	2.9	6.6	2.2	4.2	2.0	1.3	16.3	42.7	0.4	1.0
10C	--	672.0	2.2	337.0	4.0	12.8	1.5	85.0	2.5	1.8	1.8	1.2	12.0	1109.8	0.3	25.4
11C	5.4	4.0	4.2	3.7	0.8	7.1	1.7	6.9	2.5	1.8	2.2	4.2	16.8	27.7	0.4	0.6
12C	7.4	4.2	4.5	4.4	0.8	8.7	1.5	6.9	1.8	1.5	2.2	7.4	18.2	33.1	0.4	0.2
13C	20.3	273.5	5.0	4.0	2.2	26.5	2.5	31.4	49.9	6.6	131.9	54.4	211.8	396.4	4.8	9.1
14C	3.0	41.8	1.8	56.6	0.3	13.9	2.0	9.4	6.0	3.0	2.2	1.8	15.3	126.5	0.4	2.9

TABLE X.1

Sub-array	JAN (5) >20	>200	FEB (4) >20	>200	MAR (4) >20	>200	APR (4) >20	>200	MAY (5) >20	>200	JUN (4) >20	>200	Total ½ year >20	>200	Per cent ½ year >20	>200
01A	5.9	--	0.3	0.3	0.8	0.7	--	0.3	1.2	0.7	0.3	--	8.5	2.0	0.2	--
01B	4.2	0.3	1.7	0.3	1.8	1.3	0.3	0.3	1.5	0.7	0.3	--	9.8	2.9	0.2	0.1
02B	5.2	--	1.7	15.6	1.2	1.3	0.7	1.0	2.2	3.7	0.3	--	11.3	21.6	0.3	0.5
03B	4.5	--	1.0	15.6	1.8	1.3	0.7	1.0	3.0	45.5	0.3	--	11.3	63.4	0.5	1.5
04B	6.0	--	1.3	--	1.5	1.3	0.3	0.3	1.8	1.5	0.7	--	11.6	3.1	0.5	0.1
05B	125.8	85.3	83.5	43.0	90.7	148.3	3.4	32.4	1.8	10.4	0.3	1.2	305.5	320.6	7.0	7.3
06B	26.9	4.0	8.2	24.7	1.8	9.7	8.6	34.3	4.5	11.2	0.3	1.2	50.3	83.1	1.2	1.9
07B	4.7	234.0	5.4	22.2	3.0	6.6	3.9	33.6	2.5	18.9	--	1.2	19.5	316.4	0.4	7.2
01C	22.2	153.2	12.3	36.3	2.5	6.7	--	640.8	--	840.0	--	672.0	37.0	2349.0	0.8	53.8
02C	5.0	1.0	3.9	6.6	3.7	1.7	199.2	199.8	4.9	22.3	--	--	216.7	231.4	5.0	5.3
03C	5.7	--	--	0.3	2.4	1.8	0.3	0.7	1.5	3.0	0.7	--	10.6	5.8	0.2	0.1
04C	4.5	0.3	0.3	24.9	1.2	1.3	1.0	0.3	1.8	3.5	1.0	--	9.8	30.3	0.2	0.7
05C	3.7	--	1.3	16.8	0.8	2.7	1.2	1.5	1.8	1.3	0.3	--	9.1	22.3	0.2	0.5
06C	3.9	--	0.7	126.2	1.5	9.6	--	1.3	1.2	1.5	--	--	7.3	138.6	0.2	3.2
07C	15.1	9.4	1.0	--	2.9	0.3	0.3	--	2.2	3.9	6.2	143.0	27.7	156.6	0.6	3.6
08C	3.5	30.7	1.5	2.9	0.3	--	--	0.8	--	--	--	58.6	5.3	93.0	0.1	2.1
09C	9.9	46.7	16.3	47.7	2.9	6.7	21.8	36.5	4.4	18.5	11.4	16.8	66.7	173.0	1.5	4.0
10C	54.4	5.5	8.4	41.5	2.2	82.7	19.3	38.0	6.0	14.1	5.2	115.1	95.5	296.9	2.2	6.8
11C	33.8	3.0	18.3	28.9	2.5	7.1	9.1	92.2	1.8	36.3	1.3	--	66.8	167.5	1.5	3.8
12C	32.3	2.9	9.6	51.4	1.7	6.7	8.2	35.8	51.9	53.8	1.5	--	105.2	150.6	2.4	3.4
13C	302.4	48.6	122.8	122.8	2.4	115.6	6.4	194.5	0.7	36.1	0.3	--	435.0	517.6	10.0	11.8
14C	23.7	5.0	28.1	28.1	2.2	4.9	13.6	37.3	2.7	5.0	0.3	--	70.6	80.3	1.6	1.8

TABLE X.1

Sub-array	TOTAL YEAR >20	>200	PER CENT YEAR >20	>200
01A	16.7	6.9	0.2	0.1
01B	21.6	9.5	0.2	0.1
02B	19.4	57.5	0.2	0.7
03B	19.0	69.4	0.2	0.8
04B	19.7	17.3	0.2	0.2
05B	465.8	355.9	5.3	4.1
06B	68.7	112.0	0.8	1.3
07B	40.8	432.1	0.5	4.9
01C	49.6	2536.0	0.6	29.0
02C	283.2	251.2	3.2	2.9
03C	26.2	100.4	0.3	1.1
04C	16.9	159.3	0.2	1.8
05C	16.7	427.5	0.2	4.9
06C	12.9	245.7	0.1	2.8
07C	145.9	170.3	1.7	1.9
08C	27.2	141.9	0.3	1.6
09C	83.0	215.7	1.0	2.5
10C	107.5	1406.7	1.2	16.1
11C	83.6	195.2	1.0	2.2
12C	123.4	183.7	1.4	2.1
13C	646.8	914.0	7.4	10.5
14C	85.9	206.8	1.0	2.4
AVERAGE	108.2	373.4	1.2	4.3
LESS 01C		270.4		3.1

Y. ARRAY MONITORING AND FIELD MAINTENANCE

This section includes a review of actions of remote array
monitoring at NORSAR Data Processing Center (NDPC) and
maintenance accomplished at the subarrays and the NORSAR
Maintenance Center (NMC) by the field technicians.

Y.1 Subarray Monitoring Schedule

The planned schedule for the remote array monitoring (AM)
has been well met. No changes have been made in the schedule
in the reporting period. The schedule is presented in Table
Y.1. The off-line computer requirement for AM is on the average
approximately 20 hours per month. Including the on-line
tests, the on-line computer time requirement is approxi-
mately 77 hours.

TABLE Y.1

Monitoring rates for AM programs.

Biweekly	Monthly	Bimonthly	Quarterly	Annually
LPCAL	SLEMTEST	MISNO	CHANEVLP	SACPLP
RSA/ADC		CHANEVSP		
Test		SACPSP*		

*Subarrays with newly overhauled seismograph ampli-
fiers are analyzed every four months.

Y.2 Maintenance Visits

Fig. Y.1 shows the number of visits to the different
subarrays in the period. Excluding visits caused by troubles
in the communications system, the subarrays have on the average
been visited 7.5 times. The large difference from average
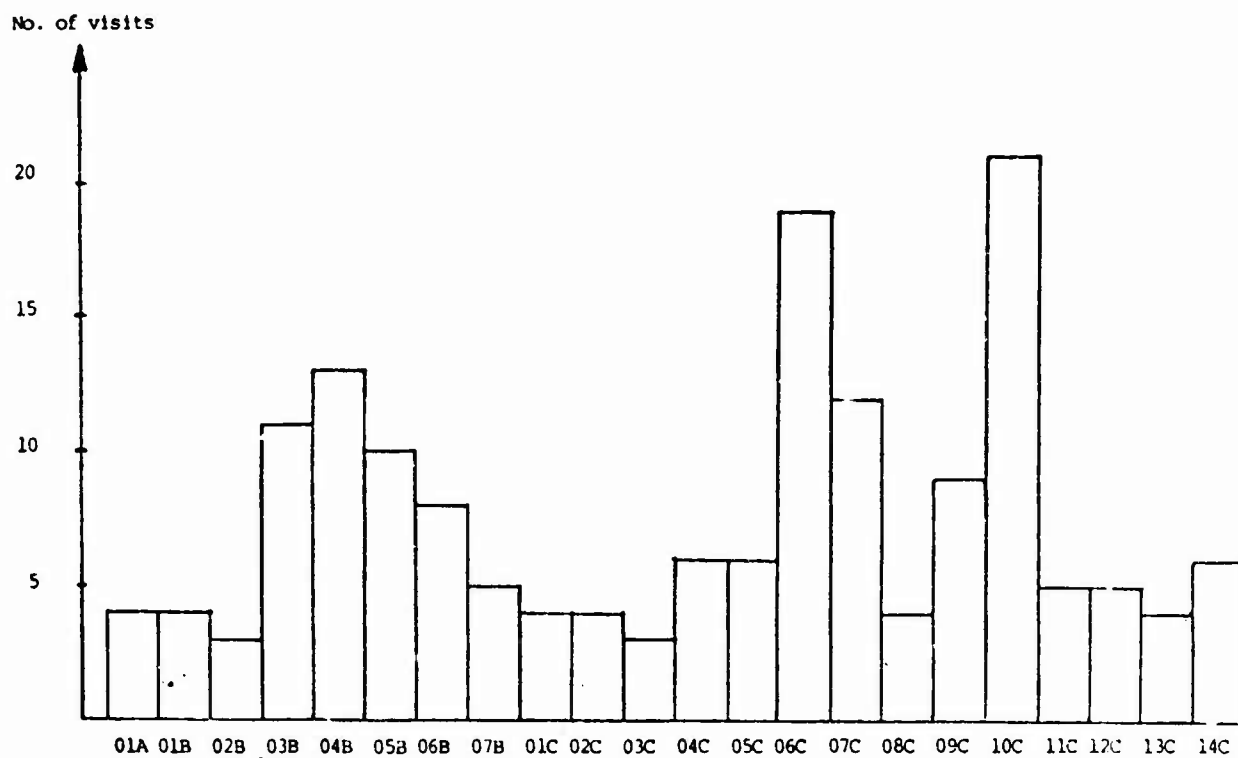for subarrays 03B, 04B, 06C, 07C and 10C is explained in
Table Y.2.

Fig. Y.1   Number of maintenance visits to the NORSAR subarrays
             1 July 1974 - 30 June 1975.

TABLE Y.2

Tasks accomplished at 03B, 04B, 06C, 07C and 10C

Sub-array	No. of Visits	Maintenance Visits on:					Comments
		Power/ rectifier	Cable breakage	LP ch's incl. RCD	BE Card	Other Maint.	
03B	11			8		3*	* LTA discrepancies and ch. gain adj.
04B	13		4	3	1	5*	* 2 RA-5's with distortion (3 visits) and CMR/ch. gain.
06C	19	2	5	3	5	4*	* Faulty RA-5's (3 visits) EM cal. circuit faulty
07C	12	1	4		3	4*	* RSA/ADC faulty (1 visit) DCO unadjustable and ch gain (2 visits). RA-5 faulty.
10C	21		16		2	3*	* Routine replacement of RA-5's to prevent power decay (2 visits). Test generator faulty.

Y.3 Preventive Maintenance Projects

Work accomplished as part of this type of the preventive
maintenance of NORSAR is described in Table Y.3. The work
at WHVs consisted of maintenance such as painting of the
wood frame, replacement of RA-5 amplifiers and control of
all circuits at the site. The new RA-5's installed had
been fully overhauled with new power batteries mounted.

TABLE Y.3

Preventive maintenance accomplished at NORSAR during the period.

Unit	Action	No. of Channels Accomp.	Remaining	Comments
SP Seism.	Adjustment of damping	3	–	10C06,02C05,06 (10C03 remaining from last period has drifted within tolerance limits).
RA-5	Modification of RA-5 input card	1	1[1]	10C04 (remaining 12C05)
LTA	Adjustment of SP DC offset to positive bias[2]	94	–	Whereof 4 LP ch.
	Modification of DC offset adjustment range (R12)[2]	102	0	Remaining: 04B, 01C,08C,13C,14C.
WHV and RA-5	Construction maintenance	11	9	04C03,04,10C01,02, 03,04,06, 02C03,04, 05,06
	RA-5 replacement	10	11	10C01-06, 02C03, 04,05,06 (remaining:12C01-03,05,06, 14C)

[1] Modified for noise supression, but variable damping resis-
tance is lacking.

[2] Refer Larsen and Nilsen, 1974.

Y.4 Disclosed Malfunctions on Instrumentation and Electronics

Table Y.4 gives the number of accomplished adjustments
and replacements of field equipment in the total array
with the exception of those mentioned in Table Y.3.

TABLE Y.4

Total number of required adjustments and replacements in the NORSAR
data channels, 1 July 1974 to 30 June 1975.

Unit	Characteristic	SP Repl.	SP Adj.	LP Repl.	LP Adj.
Seismometer	Damping		3		7
	Nat. Freq.	2			
	Sensitivity	1			
	Distortion				
	RCD			18	4
Seismometer Amplifier PA-5	Gain	2	2		
	Distortion	2			
	Cal.amp.inop.	2			
LTA	Ch gain	1	45		3
	Filter discr.	12			
	DCO	4	12		
	CMR	2	9		
	K2 relay fault	4			
BE card		43			
SLEM					
BB gen.		3	2		
SP gen.		1			
LP gen.		1			
RSA/ADC		2	5		
EFU		1			
DU			1		

Y.5   Malfunction of Rectifiers, Power Loss, Cable Breakages

Malfunction of the rectifiers and power loss requiring
action of the field technicians are reported in Table
Y.5.

TABLE Y.5

Faults disclosed in subarray rectifiers

and power loss.

Sub-array	Fault	Period of inoperation	Comments
02B	Main AC power break	8-9 Dec	
01C	Rectifier failed to go into "High Charge" battery power low.		Restarted manually
06C	Main AC power break		Main fuses replaced
	-"-	4-5 Mar	
07C	Rectifier continuous in "High Charge"		Timer coil burned
10C	Main AC power break		Main fuses replaced
14C	Rectifier trafo M2 burned, diode failure on M2 card.	10-13 Aug	

In the period 27 cab.e breakages have occurred in all types
of cables. The field maintenance personnel spent 77 days'
work on 17 of the breakages, the rest were repaired by
NTA. The status as of 30 June was:

01C: Power cable broken 31 March 75. Repair will be com-
pleted in August 75 including modification from
10 KV to 1 KV network.

07C: 04 cable broken 24 March. Repair has been delayed
due to agricultural activity. Approximately 600 meters
of cable have to be spliced in and buried in a depth
of two meters.

09C: 03 cable broken by lightning 16 June 75.

10C: 04 cable was broken again 30 April after repair 14 March
75. 05 cable has been broken since 2 October 74. After
8 days' work the repair had to be postponed due to
bad snow conditions. The cable repair is expected to
be time-consuming, but should be completed in July 75.

Y.6 Workshop Repairs

All units removed from the field (refer Repl. columns in
Table Y.4 and Table Y.3 - RA-5 replacement) this and
previous reporting period have been repaired, with the
exception of a few SP seismometers. Also remaining un-
repaired at NMC are:

    1 DC/DC converter
    6 RA-5 input cards
   11 BE protection cards
    1 Code Converter 02

Thirteen LTA cards with presampling filter faults are
stored at NMC. Repair (replacement of the presampling
filter) is not planned in the near future, as the number
of spare LTA cards is good.

Y.7 NMC Facilities and New Instruments

The NMC workshop and storage were slightly damaged by fire
24 November 1974. The cleaning up and repair work engaged
the field technicians several weeks. The communication line
between NDPC and NMC was broken during the fire and has
not been re-established. In order to save funds investiga-
tions were initiated to achieve alternative solutions to
the permanent line. After installation of the short period
analog SP station at NMC/04B05 there is a two-pair line
connection between NMC and the CTV at 04B through 04B05.
The experiments and measurements made are promising, but
line equilizers should be constructed before the line may
be taken in regular use.

One Hewlett-Packard 5035T logic lab including logic test probes were acquired in April 1975.

Y.8 Improvements

The status of a number of investigations to prepare lasting solutions to problems or time-consuming maintenance of certain units experienced during the operation of NORSAR is as follows:

- Depression of noise in SLEM discrete inputs and
- Too low surge rating of BE protection card

- False triggering of CTV water monitor

- Trends towards negative DC offset in the SP/LTA

Proposed modifications have been tested and are described in Larsen, Falch and Pettersen, 1975. We are now awaiting approval. Investigations have shown that only marginal improvements can be gained by a modification. Recheck of the "turn on" point is expected to be completed on all subarrays this year. Modification (refer Larsen and Nilsen, 1974) is accomplished on 77% of the channels.

Y.9 Short Period Analog

The short period analog station located at subarray 05C with the recording drum in the NORSAR Data Processing Center (NDPC) was moved to the subarray 04B/NORSAR Maintenance Center (NMC) in November 1974. The recording station is placed in a room in the office building at NMC, the seismic signals are received from seismometer 04B05 with a separate RA-5 seismometer amplifier through a buried cable. The

station is operated continuously and the seismograms
are forwarded to NDPC once a week. The technical layout
is given in Larsen, 1975. Note that explanations to the
Figs. 1 and 2 in the report are interchanged.

Y.10 Experimental Broadband Analog (Kirnos)

The cooperative Nordic research project involving the
operation of a Kirnos station at NORSAR concluded 20
September 1974, and the instrumentation was re-shipped to
Finland 30 October. The installation and calibration of
the instrument are described in detail by Pettersen and
Larsen (1974). An evaluation of the station is given in
section M in this report.

Y.11 Conclusion

Except for one remark described below, the field instru-
mentation has operated satisfactorily throughout the period
and the facilities are in good standard. Compared with the
previous year (refer Bungum, 1974a and b) an increasing
number of replaced LP RCD's is observed. The most common
fault is corrosion and rust on the RCD's caused by moisture
in the LP tanks making the RCD's immovable. But otherwise
there has been less moisture in the LPV's after implementa-
tion of the routine of not visiting the LPV's except for
corrective maintenance. The cause of the damping ratio of
the LP channels which have an increasing trend is planned
investigated next year. The SLEM units have been more stable
this period compared with the previous period, also the
number of burned out BE protection cards has been less
(43 compared with 68).

The preventive maintenance program for the WHV's and RA-5's
has been delayed as priority has been given to the corrective
maintenance. Eleven channels are now remaining and will
be completed this summer.

The array average DC offset of the SP channels which was
nominal one year ago is now plus one quantum unit and is
explained by the fact that the modification program of
the DC offset trim range of the LTA's is nearly completed.
The offset is adjusted to a positive bias of three milli-
volts to compensate for the negative trend. Because of
relatively high noise level the short period data from
subarray 14C has been masked since 16 May.

<div align="right">Alf Kr. Nilsen</div>

REFERENCES

Bungum, H. (1974a): Semiannual Technial Report, NORSAR Phase 3,
      NORSAR Scientific Report No. 4-73/74, NTNF/NORSAR, Kjeller,
      Norway.

Bungum, H. (1974b): Semiannual Technial Report, NORSAR Phase 3,
      NORSAR Scientific Report No. 6-73/74, NTNF/NORSAR, Kjeller,
      Norway.

Larsen, P.W. (1975): Reinstallation of NORSAR SP Analog Station
      (NAS), NORSAR Internal Report No. 5-74/75, NTNF/NORSAR,
      Kjeller, Norway.

Larsen, P.W., and A. Kr. Nilsen (1974): DC offset trim modification
      of NORSAR short period line terminating amplifier, NORSAR
      Internal Report No. 8-73/74, NTNF/NORSAR, Kjeller, Norway.

Larsen, P.W., K. Falch and R. Pettersen (1974): Modification proposals
      on SLEM and associated equipment, NORSAR Internal Report No.
      3-74/75, NTNF/NORSAR, Kjeller, Norway.

Pettersen, R., and P.W. Larsen (1974): Installation and Calibration
      of KIRNOS instrumentation, NORSAR Internal Report No. 7-73/74,
      NTNF/NORSAR, Kjeller, Norway.

ABBREVIATIONS

AC	- -	Alternate current
ADC	-	Analog-to-Digital Converter
BB	-	Broad band
BE Card	-	Lightning Protection Card
CMR	-	Common Mode Rejection
CTV	-	Central Terminal Vault
DC	-	Direct current
DCO	-	DC offset
DU	-	Digital Unit
EPU	-	External Power Unit
LP	-	Long period
LPV	-	Long Period Vault
LTA	-	Line Terminating Amplifier
NTA	-	Norwegian Telegraph Administration
RCD	-	Remote Centering Device
RSA	-	Range Scaling Amplifier
SLEM	-	Seismic Short and Long Period Electronics Modules
SP	-	Short period
WHV	-	Well Head Vault